Eugene E. Lundquist

ARR Apr. 1942

NATIONAL ADVISORY COMMITTEE FOR AERONAUTICS

WARTIME REPORT

ORIGINALLY ISSUED

April 1942 as
Advance Restricted Report

A METHOD OF SHEAR-LAG ANALYSIS OF BOX BEAMS FOR AXIAL STRESSES, SHEAR STRESSES, AND SHEAR CENTER

By Oscar Erlandsen, Jr., and Lawrence M. Mead, Jr.
Grumman Aircraft Engineering Corporation

NACA

WASHINGTON

A METHOD OF SHEAR-LAG ANALYSIS OF BOX BEAMS FOR AXIAL STRESSES, SHEAR STRESSES, AND SHEAR CENTER

By Oscar Erlandsen, Jr., and Lawrence M. Mead, Jr.

SUMMARY

A practical and relatively rapid method of compensating for shear lag in box-beam analysis, with accuracy sufficient for design purposes, is presented. Effectiveness curves for box-beam elements are derived for an ideal, symmetrical structure. Application of the ideal curves to practical structures is described in detail using, as examples, the center section of the wing for an airplane designated as A and the unsymmetrical D-beam of the wing for an airplane designated as B.

Tabular computation forms for rapid, accurate calculation of axial stresses, shear center, and shear stresses for a beam with shear lag are included. Results of analysis are compared with test stress distributions. Analytical methods of checking the shear-lag curves by the use of the principle of consistent deformations are illustrated as a further indication of their reliability.

INTRODUCTION

Bending stresses in box beams with thin cover sheets usually differ from those calculated by the ordinary bending theory. This difference is caused primarily by shear deformation in the flanges or cover sheets. In order to compensate for differences from the theory, methods of shear-lag analysis have been developed.

Kuhn (references 1 to 5) has done much mathematical and experimental work on idealized structures under simple loading conditions and has developed two methods of shear-lag analysis - the substitute single-stringer method and the shear-fault method - that approach the problem by means of arithmetic integration. This approach gives fairly accurate results for beams that are fairly symmetrical.

As the beam becomes more unsymmetrical, however, with possibilities of changes of taper, camber, variable sections, discontinuous stringers, holes, and indeterminate boundary conditions and as the loading pattern becomes less

simple, the NACA methods become more difficult to apply. The computation is very tedious and of dubious accuracy where there are excessive approximations required of the designer in idealizing the structure so that it will fit the method. Furthermore, the NACA methods require two separate analyses for beam and chord bending, which considerably lengthens the calculations.

From design considerations, it is desirable to have a simple flexible method of shear-lag analysis that can be tailored to the individual conditions of any wing beam. It should require a minimum of idealization of sections so that irregular beams may be readily analyzed and should, if possible, enable a simultaneous consideration of beam and chord bending. It should be possible to check the results of the analysis in a simple straightforward fashion.

The method of shear-lag analysis herein presented was developed by the Grumman Aircraft Engineering Corporation in the course of recent designs and, it is believed, incorporates these desirable features.

OUTLINE OF METHOD

Essentially, the method consists in applying a correction for shear lag to the areas of a beam cross section and then analyzing the substitute beam by the conventional bending theory. A check for the shear-lag correction can be made if desired.

(1) Shear lag reduces the effectiveness of cover sheet and stringers for carrying bending stresses. Consequently, stresses in the cap strips will be raised and stresses in the stringers will be reduced from those computed by the ordinary beam theory. If the stringer stress at a section decreases 20 percent and the cap-strip stress increases 10 percent from the theory, the effectiveness factor E' for the stringer will be $100 - 10 - 20 = 70$ percent, referred to the beam theory cap-strip stress as 100 percent.

Effectiveness curves are drawn in chordwise and spanwise directions for each stringer and wing section by taking mathematically ideal curves and altering them arbitrarily to suit local conditions in the structure. Care must be taken that the location of the centroid of the effective material, and hence the shear center, varies in a smooth

spanwise curve. Common sense, cross-plotting, and a few rough checks will give surprisingly good results even with little experience in drawing such curves.

(2) Stringer and effective sheet areas are reduced by the effectiveness factor E', and section properties are computed giving reduced "effective" values for I_{xx} and I_{zz}.

(3) Axial stresses are computed by use of the method presented in reference 6 for unsymmetrical bending, modified to take the effectiveness factors into account. These stresses should give the actual stringer and cap-strip stresses compensated for the shear-lag effect.

(4) Shear stresses in the skin and webs that go with the axial stresses found in (3) can then be accurately computed by the new method. The shear center can also be accurately located and its position at the various wing sections can be checked to see that it falls on a smooth spanwise curve.

(5) The accuracy of the original selection of E' can be proved by utilizing the principle of consistent deformations. Any two points on the wing surface can be selected and the deformation of one of them from the other can be computed by two or more different paths, using the axial and the shear stresses obtained in the analysis. These deformations should agree if the values of E' were reasonably correct.

COMPARISON WITH NACA METHODS

The main difference between the effectiveness-factor method and the NACA methods of shear-lag analysis is the point at which engineering judgment is required. The NACA calls for judgment in idealizing the section before shear lag is considered. The effectiveness-factor method requires an estimate of the shear-lag effect at the outset. It is believed that in the design of new wings, the effectiveness-factor method is more direct, more rapidly applied, and comparably accurate.

In the NACA methods it is easy for the average person to lose sight of the physical significance of the problem amidst the maze of coefficients and unfamiliar formulas and to make time-consuming mistakes. The effectiveness-factor method obviates this possibility, it is felt, by its simplicity and flexibility.

(1) Once the effectiveness curves have been drawn, the analysis follows the standard beam theory. Both beam and chord bending are considered simultaneously, as described later.

(2) The method is perfectly applicable to any shape of beam because the areas of the existing structure are changed rather than the shape of the beam being idealized without changing the areas, as is done in the NACA method. It is believed that changing the area is an easier task, particularly for complex unsymmetrical sections such as D-beams, where idealization of shape would be very difficult.

(3) Local irregularities and changes in section can be readily considered by suitably drawing the effectiveness curves. Material outside the main beam may also be considered in the calculations if it is believed that it carries bending stress. This consideration would be difficult by the NACA method.

(4) Effectiveness curves give a handy tool with which to design stringer skin-rivet connections.

Analyses by both the NACA and the effectiveness-factor methods were made for a wing section of airplane A and were compared with test results. Remarkably good agreement was shown for both methods, but the effectiveness-factor method showed more adaptability to local conditions and required less computation.

EFFECTIVENESS-FACTOR CURVES

The nature of effectiveness factors and their application to shear-lag analysis will now be developed and illustrated for a simple case. A mathematical derivation of formulas for the values and the shape of effectiveness-factor curves in both spanwise and chordwise directions will be presented for an idealized beam. The method of considering beam and chord bending simultaneously with shear lag included will be outlined, and the relation between effectiveness curves and the location of the shear center in unsymmetrical sections will be discussed.

Nature of Shear Lag

Shear lag and how to compensate for it can be illustrated by consideration of figure 1, which represents the bottom surface of a wing beam from the plane of symmetry of the airplane to the hinge fittings for the outer panel. Here two loads P act on the cap strips.

The usual theory assumes that the panels will elongate as shown in figure 1(a), which would require uniform stress across the panel at all sections, even across section D. This assumption is obviously impossible because the center stringer can have no stress or axial load at its outer free end.

Actually the panel will deform as in figure 1(b) owing to the shear deflection or "lag" in the sheet. The thinner the sheet the more the lag. At the free end the stress in the stringer will be zero. As one progresses along the stringer toward the root, the load P starts to spread out into the sheet in the form of shear stresses that load up the stringer.

At the root for an infinitely long panel the stress in the stringer would be equal to that in the cap strips and there would be no shear stress in the sheet and no shear lag.

It is important to realize that the stringer can be loaded only by shear from the sheet. If the panel is short or the sheet very thin, the sheet will not be able to transmit enough load to the stringer to stress it at the root to the same amount as the cap strip (as would be figured from the ordinary beam theory). This case is usually true for wing box beams.

Hence, it is seen that the stress in the stringer varies from zero to some maximum value at the root; this value depends on the dimensions of the beam. Compared with the uniform stress of P/A calculated from the beam theory, the stringer is operating at a reduced stress, or reduced effectiveness, that varies on some smooth curve from $E' = 0$ at the free end to $E' =$ maximum at the root. Likewise the cap-strip stress will vary from a maximum value of the free end to a minimum value of the root.

These deviations from the beam-theory stress may be obtained from figure 2.

At section C of figure 1(b), let it be assumed that with shear lag the stringer stress will be half of that computed by the P/A formula (fig. 2). The value of E' for the stringer would be 0.50 and for the cap strips would be slightly greater than 1.00. It is convenient, however, always to assume the E for the cap strips to be unity.

The effectiveness E' for a stringer will be defined as the effectiveness of the stringer for carrying stress as compared with the cap strip. This definition will make E' for the stringer slightly less than 0.50, say 0.43. If the effectiveness factor for each member is applied to the area of the member, an effective area is obtained.

Effective area = $(3\times1.00)+(2\times0.43)+(3\times1.00)=6.86$ square inches

Shear-lag stress in any member = $\frac{P}{A_{effect}} \times E'$

For cap strip $\frac{20000}{6.86} \times 1.00 = 2920$ pounds per square inch

For stringer $\frac{20000}{6.86} \times 0.43 = 1254$ pounds per square inch

Beam-theory stress = $P/A = \frac{20000}{8} = 2500$ pounds per square inch

$$\frac{\text{Shear-lag stringer stress}}{\text{Beam-theory stringer stress}} = \frac{1254}{2500} = 0.50$$

This result checks the original assumption. It is possible, therefore, to take shear lag into account by selecting effectiveness values for each element of the cross section. The component areas are corrected by these factors, and from there on the calculation is similar to that for the ordinary beam theory. The actual value of the effectiveness factors selected will be governed by the mathematical derivations to be discussed later.

Mathematical Derivation of Spanwise Curves

A box-beam cover is statically indeterminate internally to the first degree; therefore, with two static relationships and one elastic relationship, it can be solved. The symbols are defined in appendix A. From these three

fundamental equations, differential equations for f_F, f_L, and f_s can be derived in terms of the physical constants and the loads of the problem. These differential equations can be solved mathematically for simple loadings and symmetrical sections. The ratio of f_L to f_F will be the effectiveness factor for the stringer member in terms of the cap strip.

The sketch of figure 3 shows the idealized beam with applied moments and shears. The material in the bottom of the beam can be considered to be concentrated entirely at the bottom flanges. The origin of the coordinates is taken at the tip. (See reference 1.)

Effectiveness-factor curves for the idealized beam sketched in figure 3 will be mathematically derived. The following assumptions are made in the derivation:

1. Ribs, and hence beam, have infinite chordwise stiffness so that chordwise strains may be neglected

2. Diagonal tension in the sheet is taken care of in factor G

3. Sections and loads are symmetrical about the yz plane

Fundamental equations.- Consider the static equilibrium of the element dy (fig. 4 and reference 1). It will be seen that

$$dP_L = dS_L \tag{1a}$$

$$dP_F = \frac{S_W dy}{h} - dS_C \tag{1b}$$

From assumption (1) and figure 5, it follows that the shear stress

$$f_s = \frac{G}{b} (\Delta F - \Delta L)$$

but

$$L = \int_{y=L}^{y=y} \frac{f_L \, dy}{E}$$

and

$$F = \int_{y=L}^{y=y} \frac{f_F \, dy}{E}$$

and, by differentiation,

$$df_s = - \frac{G}{Eb} (f_F - f_L) \, dy \qquad (1c)$$

Effectiveness factor.- Equations (1a), (1b), and (1c) can be combined into four differential equations for f_F, f_L, and f_s. (See appendix B for detailed derivations.) For the beam in figure 3 the equations for f_F and f_L can be solved to be

$$f_F = \frac{M}{A_T h} \left[1 + \frac{A_L}{A_F} \frac{\cosh K (L - y)}{\cosh KL} \right] \qquad (2a)$$

$$f_L = \frac{M}{A_T h} \left[1 - \frac{\cosh K (L - y)}{\cosh KL} \right] \qquad (2b)$$

where $M/A_T h$ is the ordinary beam-theory stress and the term in the bracket is the effectiveness factor of each referred to the beam-theory stress as unity. Since the E' for the flange, or cap strip is taken as 1.00 for convenience, the actual E' for the stringer referred to the cap strip will be

$$E' = \frac{f_L}{f_F} = \frac{1 - \frac{\cosh K (L-y)}{\cosh KL}}{1 + \frac{A_L}{A_F} \frac{\cosh K (L-y)}{\cosh KL}} \qquad (3)$$

where K, the shear-lag parameter, equals $\sqrt{\frac{Gt}{Eb} \left(\frac{1}{A_F} + \frac{1}{A_L} \right)}$ and the other symbols are defined in appendix A. Equation (3) is plotted in figure 6 for various values of K and L

Limitations and Application of Spanwise Curves

Multistringer beams.- Equations (2b) and (3) are for

a single-stringer beam. When there is more than one stringer, the usual case, the stringers between the cap strip and the shear center should be lumped into a single stringer at the area centroid of the stringers, a distance b from the cap strip, before K is computed. This method will give a good approximation of the average E' for the stringers for a fairly symmetrical box beam. The chordwise distribution between these stringers will follow the shape of the chordwise curves discussed later.

For very unsymmetrical beams, such as D-beams, values from equations (2b) and (3) will be only very approximate, but the general shape of the curves will always hold and the values can best be obtained from consideration of the location of the shear center and the center of gravity of the effective material.

Variable sections.- Equation (3) is strictly true only if, at each spanwise station, the following conditions hold:

(a) Constant $K^2 = \frac{Gt}{Eb}\left(\frac{1}{A_F} + \frac{1}{A_L}\right)$

(b) Constant A_L/A_F and no camber

(c) Constant beam-theory axial stress $M/A_T h$

(d) Constant vertical-web shear stress S_W/ht

Conditions (c) and (d) are sought for in practical wing design and condition (b) is usually fairly nearly true. Condition (a) is seldom satisfied for a tapered variable-section wing but, by the use of an average value for the panel, the error will not be large and judicious fairing of curves will give results accurate enough for design purposes.

Riveted joints.- For a constant-section stringer, the slope of an effectiveness curve such as shown in figure 6 represents to some scale the change in axial load per inch of span. This value is the design load for rivet spacing between stringer and skin and will be critical at the free end of the stringer where the slope is steepest. Since for most wings the curves will not be precise, the 1.20 fitting factor should not be omitted in the design of rivets based on effectiveness curves. The curves of figure 6 are critical for stringers but are not critical for rivets; the 1.20 fitting factor will cover any divergence.

Mathematical Curves for Chordwise Effectiveness

In references 1 and 2 analytical solutions have been made that show the chordwise distribution for ideal beams with a cover sheet without stiffeners (or infinitely closely spaced stiffeners). This distribution follows a hyperbolic cosine law

$$f = f_F \frac{\cosh\left(Yb \frac{x}{b}\right)}{\cosh Yb} \tag{4}$$

where f_F is the stress in the cap strip ($x = b$) and Y is an auxiliary parameter obtained from the relation

$$\frac{\tanh Yb}{Yb} = \frac{f_L}{f_F} \tag{5}$$

where f_L/f_F is the ratio of the stress in the stringer material located at the stringer force centroid to the stress in the flange. Figure 13 of reference 1 is a curve presented to facilitate solution of equation (5). The ratio of f/f_L from equation (4) will be the effectiveness of any stringer in terms of the cap strip or flange. Curves of f/f_L for various values of Yb or f_L/f_F are presented in figure 7.

Limitations and Application of Chordwise Curves

In general, the mathematical curves of chordwise effectiveness are not strictly accurate, because

(1) Most wings have a finite number of stringers and will not follow equations (4) and (5) exactly

(2) Local conditions, dissymmetry of section, etc., will vary curves

The theoretical curves, however, will give the general shape of chordwise curves and also will give a point of departure from which to correct for the local conditions of the problem.

Curves for Simultaneous Beam and Chord Bending

The previous discussion has dealt with effectiveness curves for bending in only the beam direction. Wing beams are subjected to both beam and chord bending. For the box beam shown in figure 8 the chordwise-effectiveness curves for beam and chord bending are shown and it will be noted that they are not the same. For a precise analysis, this difference means that there are two different beams with different areas corresponding to the two effectiveness curves. The beams must be separately analyzed for beam and chord bending, which would be very tedious.

If a single value of effectiveness for both beam and chord bending can be selected, the beam may be analyzed by the unsymmetrical-bending formula. This will be done by using the beam-effectiveness curve as the true total effectiveness of the beam. The error introduced will be small for the following reasons:

(1) The chord moment, at the most, is only about one-third of the beam moment and it is usually less than this.

(2) For the beam of figure 8, where the beam and the chord effectiveness of members b and c near the chord neutral axis differ markedly, the stresses due to chord bending will be small and the errors even smaller. This result is true in most box-beam sections.

(3) Material back of the main beam is usually ineffective in beam bending but quite effective in chord bending. In order to take care of this condition, the effectiveness factor E' will be selected from consideration of chord bending and the z coordinate of the material will be assumed to be zero, so that the terms will drop out of the beam-bending calculations just as though the beam effectiveness were zero, but will not drop out of the chord calculations.

(4) Where beam effectiveness is very low and chord effectiveness is high, the value of the effectiveness factor E' can be slightly increased over the value for beam effectiveness in order to compensate in part.

A little thought and care in evaluating the relative chord and beam effects will give effectiveness curves that are sufficiently accurate for design purposes.

RELATION OF SHEAR CENTER TO EFFECTIVENESS CURVES

In symmetrical sections the ideal curves of figures 6 and 7 are usually sufficient guide for obtaining fairly accurate results. In unsymmetrical sections such as D-beams, however, the ideal curves give a guide as to the shape of the curves but are of little service in selecting the values, because it is nearly impossible to get an accurate value of K with which to enter the curves. The location of the shear center and the centroid of the material effective in bending are used as guides in drawing effectiveness curves for such beams.

Shear-center location.- The shear center, s.c., of a section shall be defined as the point at which any load may be applied to the section without tending to twist the section. Only pure bending will occur. (It should be noted that the sheer center is not necessarily the same as the elastic axis about which the section twists.) For a symmetrical section the shear center will coincide with the centroid of the section. For unsymmetrical sections, however, the resultant of the shear forces on the section does not pass through the centroid. (See fig. 9.)

The point s.c. is so located that the moment of the shear forces about s.c. is zero. Any load applied through point s.c. will cause pure bending in the direction of the load. Reference 6 shows that for a D-beam section the shear center s.c. lies as shown in figure 9(c), inside the closed torque box and not far from the centroid. The heavier the vertical web becomes with respect to the skin sheet thickness, the closer the shear center will move toward the web.

Shear center with shear lag.- The presence of shear lag is taken care of by a reduced effectiveness for the area of material other than at the cap strip. In a D-beam this reduction will move the centroid of the effective area closer to the web than was the centroid of the total area and hence closer to the shear center. For sections with closed torque boxes it will be assumed, therefore, that the shear center and the centroid of the effective material coincide and fall within the torque box. This assumption is only approximate but the error introduced is small. The assumption is a useful one, because rules that apply to the location of the shear center can be applied to the centroid of the effective areas and will serve as a control on the shapes of the effectiveness curves selected.

Motions of shear center.- With most common box sections, it is generally true that the shear center cannot suddenly change its chordwise location from one spanwise section to the next. To do so would introduce a large change in torque on the beam that would require special construction not usually found in such sections; therefore, the shear center, and with it the centroid of the effective material, follows a very easy spanwise curve.

In the sketch of the box beam shown in figure 10, the shear center at the built-in end and at the free end will be on the center of gravity because of symmetry at these points. Between these points the shear center will not follow the center line of the section but will take a smooth curve as shown, crowding the inside corner. At section A-A, therefore, the effectiveness must vary as shown in the sketch in order to keep the shear center where it should be. This result raises the stresses in the corner, a well-known phenomenon.

This law is used by drawing effectiveness curves such that the center of gravity of the effective material follows a smooth easy spanwise curve such as the shear center would take. It will be found that this requirement will give fairly definite values for the effectiveness at any point.

EXAMPLES OF EFFECTIVENESS CURVES

Sample effectiveness curves for wings of two airplanes, airplane A and airplane B will be drawn. Calculations for the corresponding stresses were made for the wing of airplane A (not included herein) and comparison with test results will be made. For the wing of airplane B, sample calculations will be included to illustrate the standard forms that have been developed for rapid wing analysis.

Wing Beam of Airplane A

Center section.- Shear-lag effectiveness curves will be drawn for the wing of airplane A from stations 18 to 110. Figure 11 shows a typical cross section and plan. Inboard of station 18 the section will be considered stiff enough to neglect shear lag, because of the 0.081-inch doubler plate (later altered to 0.102 inch but here kept at 0.081 inch

for comparison with tests). Outboard of station 110 there is a large hole in the top that will be considered. Material ahead of and back of the main box beam will be considered ineffective and will be neglected. Effectiveness factor E' is plotted for the top cover in figure 12.

The effectiveness in chord bending would be unity throughout the cover but, as stated previously, the stresses due to chord bending will be small and the curves will be drawn according to beam bending only. Because of symmetry, the shear center of the original section will be approximately at the center of gravity of the section. Shear lag will not appreciably move the shear center and a detailed study of these motions will be unnecessary in this simple structure. (See airplane B D-beam treated later for the case in which shear-center location is significant.)

Effectiveness factor determination for top surface.- The effectiveness factor for the top surface can be determined as follows:

1. Stringer D -

Find spanwise-effectiveness distribution for stringer D

At station 18, $E' = 0$

At station 110, $E' = 0$ because of hole beyond these points

To approximate E' at station 66, compute for this section

$$K^2 = \frac{Gt}{Eb}\left(\frac{1}{A_F} + \frac{1}{A_L}\right)$$

$\frac{G}{E} = 0.40 \quad t = 0.156 \quad b = 8.00 \quad A_F = 1.004 \quad A_L = 2.702$

These values were obtained from idealization of section 30-94 (fig. 11). Consider one-half width of beam and take b as the distance from front beam to center of gravity of stringers and cover plate. A_F = elements (1) + (2) + $\frac{1}{2}$(3), A_L = elements $\frac{1}{2}$(3) + (4) + (5) + (6) + (7) + $\frac{1}{2}$(8)

$$K^2 = \frac{0.40 \times 0.156}{8.00} \times \frac{1}{1.004} + \frac{1}{2.702}$$

$$= 0.0078(0.995 + 0.370) = 0.01066$$

$$K = 0.1032$$

From the curves of figure 6 the effectiveness at center of span is 0.987 for K = 0.10. Therefore, assume that E' = 92 percent at station 66 for stringer D. This value is considerably lower than 0.99 but is justified because:

a. The quantity K is very approximate owing to irregularities of section, camber, etc.

b. Curves of figure 6 are for a single stringer at center of gravity of stringer material on one-half of center line. For stringer at center line of total section, E' will be less, following smooth curve of figure 7.

Inboard of station 66, curve D can be assumed to follow very generally the shape of the idealized curve and is held high in order to take care of the increased stiffness from stations 18 to 30 because of the doubling plate. Outboard of station 66, the curve has the idealized shape but is lower than the inboard curve because of the thinner cover sheet.

2. Stringers B and F -

Stringers B and F can be considered fully effective over almost the entire length of the beam, because of their proximity to the flanges and their continuity through the plane of symmetry of the airplane. At station 126 the effectiveness will be zero because the hinge fittings of the outer panel are attached to the beams only. The effectiveness curve will stay very high until quite near station 126, so that in the region from stations 94 and 110, E' will drop only slightly.

3. Chordwise Plots -

With tentative E' curves plotted spanwise for stringers A, B, and D, chordwise plots through these stringers may be made using the shapes of ideal curves and with figure 7 as a guide.

4. Stringer C -

From the chordwise plots of step 4, the spanwise curve for stringer C may be obtained. Note that this curve is similar to that of stringer D but is slightly higher. The shape of this curve is a cross check on the accuracy of the chordwise plots.

5. Stringer E -

At station 18, E' will be very nearly equal to 1.00 because of continuity. At station 110, E' equals 0. Therefore, the curve will be as shown in figure 12. At the outboard end it will coincide with the curve for C because of the symmetry. The chordwise plots may now be completed. Bottom-surface effectiveness curves were also drawn but are not shown.

Comparison of analysis with test results.- Final stress values obtained by the effectiveness-factor method of analysis from the curves of figure 12 are plotted in figure 13 as a chordwise plot and are compared with test readings taken with Huggenberger strain gages on the actual wing surface. These test results are as reliable as test results can be expected to be, for there was no buckling in the skin nor undue distortions during the observations. Curves for the stress by the beam theory and by the NACA substitute single-stringer method of shear-lag analysis are also presented for comparison.

Agreement between test values and the effectiveness-factor method is generally very good, and it is easily apparent how to alter the effectiveness curves to improve the agreement. It was assumed that stringers B and F were fully effective and stringer E nearly so. This assumption was conservative. If the values of E' of these members were dropped slightly below 1.00, the agreement would improve. The curve as drawn, however, is sufficiently good for design purposes.

Note that, with the test results, compressive stresses tend to be lower at the front beam and higher at the rear beam than computed because of the effectiveness of the material outside the box beam, particularly for chord bending.

The NACA method for just beam bending indicates that good agreement could be had if the chord effect were superposed on it. The necessity for idealizing the section accounts for the symmetry of the curve and the lack of local irregularities that are picked up by the effectiveness-factor method. The ordinary beam theory shows good agreement only at the front beam and emphasizes the need for a quick and relatively accurate shear-lag method. The effectiveness-factor method seems to fulfill this requirement admirably.

Wing D-Beam of Airplane B

The D-beam in the wing of airplane B is quite unsymmetrical and hence compensation for shear lag is more complicated than for the ordinary box beam. In addition to having smooth effectiveness curves in chord and span directions, based on the ideal curves of figures 6 and 7, the location of the shear center and the centroid of the effective material must be made to follow a smooth curve.

A complete shear-lag analysis of this wing has been made by the Grumman Aircraft Engineering Corporation by the use of the effectiveness-factor method. In the present report a detailed description of the reasoning behind the effectiveness curves is given. Certain modifications of the curves are suggested, and new calculation forms are presented to speed up future wing analyses.

In the analysis separate curves for beam and chord effectiveness E'_B and E'_C were drawn and used in the unsymmetrical-bending formula. This method is not strictly accurate mathematically and instead the method for a single E' is recommended. In the case of the wing for airplane B, the error is insignificant because the product of inertia is very small at most sections, which would not necessarily be true of all wings.

Location of shear center.- The best place to start the shear-lag analysis is at the hinge fittings between the center section and the outer panel of the wing where the location of the shear center and loads are completely determined. (See figs. 14, 15, and 16.) For positive lift, all the tension load is carried at C (fig. 17); therefore, the shear center lies on a vertical line through C and the compression load is divided between A and B inversely as their distance from the shear center line.

Inboard of the hinge fittings, the material in the bottom cover forward of the cap strip C will start to take some of the compression load as the sheet transmits shear around from A and forward from C. This action moves the center of the compression load forward and with it the shear center. At the plane of symmetry of the airplane the shear center will be the farthest forward but, because the shear-center line must vary in a very easy smooth curve, it will not come as far forward as though there were infinite length to the center section.

Outboard of the hinge fittings the presence of the wheel well in the bottom surface prevents the compression load from distributing forward. This result keeps the shear center in line with the lower cap strip until outboard of the wheel well. From there to the tip, the shear center will move forward as the compression loads spread forward, until at the tip the shear center will coincide almost directly with the location according to the beam theory. The motions of the shear center are shown in figure 14. A method of checking the location of the shear center will later be described.

Effectiveness-factor determination for top surface.- If the assumption that the shear center and the centroid of the effective areas coincide is used as a guide and the curves are faired to look like the ideal as much as is practicable, the effectiveness curves in beam bending may be drawn. (See fig. 15.)

The cap strip B will be considered to have unit effectiveness throughout.

1. Inboard of hinge fittings -

The value of E' for stringer G will fall off rapidly as the leading edge H and stringer C build up, in order to keep the centroid of the effective material back with the shear center. At the plane of symmetry (station 0) stringers C and H will have an effectiveness of about 55 percent because it is impossible to load them any more than by means of the shear in the sheet. Stringer G will come up a little from a low point at station 44 as the shear center moves slowly forward.

The ideal curves of figures 6 and 7 are used to fair in the shape of the stringer curves. It is believed that the curve for stringer E would be improved if it were made to drop off to zero between stations 29 and 44, since it is impossible to stress the end at station 29 with more than the sheet can transmit in compression.

2. Outboard of hinge fittings -

The effectiveness of stringer G will have to fall off very rapidly through the wheel well as stringers C, D, E, F, and H build up from zero in order to keep the shear center and the centroid of effective area loads over the lower cap strip. Stringers C, D, E, and F will take

more or less ideal shapes, dying out to zero at each end. The maximum height of these curves will be governed by the condition that the shear center cannot move forward too fast outboard of the wheel well and by the rate at which the top cover sheet can transmit shear as shown by the slope of the chordwise-effectiveness curves.

Stringer H is kept very low until outside the wheel well because of the discontinuity of the torque box through this region and the nature of the curves for the under surface. Outboard of the wheel well H will gradually rise to unity near the tip as the shear forces in the sheet load it. Stringer G will drop to zero at station 277.

3. Material back of cap strip -

To neglect completely material back of the cap strip as ineffective in beam bending would introduce appreciable error, particularly for stringers near the cap strip, where it is necessary to transmit considerable shear in the sheet and riveted connections. In the analysis of effectiveness factors for beam and chord bending, the curves were as shown in figure 15. If a single factor E' is used, as is recommended for future curves, the E' for member A would follow the E'_B of figure 15. The E' for the trailing edge material (element V) would be taken equal to E'_C of figure 15, and the material would be assumed concentrated at the beam-bending neutral axis ($z = 0$) so that it would enter the chord-bending but not the beam-bending calculations.

4. Fairing in curves -

The final curves are obtained by working between the chordwise curves and the spanwise curves, with the ideal shapes and the relative effects of beam and chord bending in mind. They should show the general behavior of the top sheet without consideration for the minor irregularities that must be taken care of with more detailed investigations.

Effectiveness-factor determination for bottom surface.- The lower cap strip will be considered 100 percent effective throughout in computing the effectiveness factor for the bottom surface.

1. Inboard of hinge fittings -

Stringer J will be zero at the hinge station because the fitting is only on the top chord. It will build up as shown in order to keep shear center back where it should be.

Spanwise plots L and L' need no comment. In the chordwise plots of figure 16, however, that for station 44 seems in error. The dotted line should be followed, not the solid one, since the hole outboard of station 44 prevents stressing the sheet at this point, even in tension.

2. Outboard of hinge fittings -

In the wheel-well region, stringer J is subject to local deformations caused by the discontinuity of the torque box through the wheel well. The inclusion of these effects in the general analysis would be very difficult; the effectiveness for member J was therefore taken at zero from the hinge to station 157 for the bending-section properties and the local effects were later superimposed thereon.

Springer L has very nearly the ideal effectiveness shape, but the ideal curves would indicate that it should not come up from station 142 quite as steeply as is shown.

3. Material back of cap strip -

Effectiveness curves for the material back of the cap strip are drawn in a manner similar to that for the top surface.

COMPUTATION FORMS FOR BENDING STRESSES

Tabular forms have been prepared to facilitate computation of axial stresses and loads in wing beams; samples of the forms are included as tables 1 and 2. Table 1 shows the calculation of section properties for the effective areas. Columns 1 to 17 and computation of I_{xx}, I_{zz}, and I_{xz} need no explanation. The symbols C_1, C_2, C_3, and C_4 represent terms in the unsymmetrical bending formula altered to suit the effectiveness-factor method of analysis.

$$f_B = \frac{M_B K - M_C I_{xx}}{I_{xx} I_{zz} - I_{xz}^2} E'x + \frac{M_C K - M_B I_{zz}}{I_{xx} I_{zz} - I_{xz}^2} E'z = K_1 E'x + K_2 E'z$$

The values of K_1 and K_2 in columns 26 and 27 for each flight condition are used in table 2 to compute the bending stresses and the axial loads in each member. These load values are used in obtaining the shear stresses in the section and need be calculated only for those conditions in which the shear stresses may be critical.

SHEAR STRESS AND SHEAR CENTER

As a rough check on the accuracy of the effectiveness curves, it would be desirable to be able to find the location of the shear center in a fairly rapid, straightforward fashion. This shear center should correspond to the axial stresses and loads that were obtained from the curves.

The shear center may be found by computing the shear stresses in the sheet and the webs due only to bending and then by finding the point in the section around which the moments of these shear stresses are zero. It is an established principle that, when the axial bending stresses and loads in the members have been selected (whether rightly or wrongly makes no difference), there is only one combination of shear stresses that will maintain equilibrium. This principle has been discussed fully in references 6 to 10 and will now be discussed in detail. The principle states that, for any set of axial loads, it is possible to obtain a corresponding shear center. The spanwise curve of these shear centers will then serve as a check on the effectiveness curves, and the shear stresses obtained can be used in the design of the webs, sheet, and riveted connections.

Fundamental Equation for Shear Due to Bending

Consider the equilibrium of the element shown in figure 18 representing a portion of a box beam. Assume that the effective area of the sheet in bending is combined with the stringer. If q_n is the running shear in pounds per inch at station n, then

$$q_n = \frac{dP}{dy} + q_1$$

where dP/dy is the average change in axial load per inch in the stringer over the elemental distance dy, and q_1 is the average shear per inch over section 1.

If there are several other stringers between sections 1 and n (fig. 19), then the shear per inch at section n will be

$$q_n = \sum_1^n \frac{dP}{dy} + q_1 \qquad (7)$$

or, in terms of shear stress where $q = f_s t$,

$$f_{s_n} t_n = \sum_1^n \frac{dP}{dy} + f_{s_1} t_1 \qquad (7a)$$

The term $\sum_1^n \frac{dP}{dy}$ is easily obtained from the computed axial loads. If a load curve is drawn for each stringer and cap strip, the slope of this curve at any station will be dP/dy. A less accurate method that can be used if desired is described in reference 7; it gives the average shear over a finite length of wing. Table 3 is applicable to either method.

Derivation of Equation for Shear at Cut Section, q_1

The final value of shear flow or running shear q_n at any point due to bending alone must be such that the total shear deformation around the section from section n back to section n will be zero. Only one value of q_1 will make q_n fulfill this requirement. From the method given in references 6, 8, and 9, q_1 may be obtained by the method of least work.

Reference 10 presents a method of finding the total shear in a section, both bending and torsional, by a statically determinate method without the least-work solution. Reference 7 has amplified the method for general application in a simple straightforward fashion that completely eliminates computation of the shear center. If the shear stresses were the only consideration, this method would be the most practical. As a check on the shear-lag effectiveness curves, however, it is here desirable to be able also to find the shear center in a rapid fashion, which can be done only by making use of the least-work solution and obtaining the shear stresses, just due to bending, without the superimposed torsion. The computation is not much longer than that shown in reference 7 and the additional information obtained is worth the difference.

The least-work solution requires that

$$\frac{\partial W}{\partial f_{s_1}} = 0$$

where W is the total work due to shear deformation in the section,

$$W = \frac{1}{2G}\int_0^L f_{s_n}\, t_n\, ds$$

integrated around the complete section when $f_s t = q_s$, and

$$\frac{\partial W}{\partial f_s} = \frac{1}{G}\int_0^L f_{s_n}\, t_n \frac{\partial f_{s_n}}{\partial f_{s_1}}\, ds = 0 \qquad (8)$$

But, from equation (7a)

$$\frac{\partial f_{s_n}}{\partial f_{s_1}} = -\frac{t_1}{t_n}$$

so that equation (8) becomes

$$-\frac{1}{G}\int_0^L f_{s_n}\, t_1\, ds = 0$$

For any section, G can be considered a constant and will be assumed to include the effect of diagonal tension. Therefore

$$\int_0^L f_{s_n}\, t_1\, ds = 0 \qquad (9)$$

If equation (7a) is substituted in equation (9),

$$\int_0^L \frac{t_1}{t_n}\left(\sum_1^n \frac{dP}{dy}\right)ds + \int_0^L q_1 \frac{t_1}{t_n}\, ds = 0$$

or

$$q_1 = \frac{\int_0^L \left(\sum_1^n \frac{dP}{dy} \right) \frac{t_1}{t_n} \, ds}{\int_0^L \frac{t_1}{t_n} \, ds} \tag{10}$$

If equation (10) is substituted in equation (7),

$$q_n = \sum_1^n \frac{dP}{dy} - \frac{\int_0^L \left(\sum_1^n \frac{dP}{dy} \right) \frac{t_1}{t_n} \, ds}{\int_0^L \frac{t_1}{t_n} \, ds} \tag{11}$$

Equation (11) is perfectly general and is applicable to any single cell beam. Note that q_n is just the shear due to bending and assumes the shear loads to be acting through the shear center. Shear q_n is also the average shear flow per inch over the spanwise distance dy.

Double Cells and Other Shapes of Beams

If the box girder has more than one cell or has material extending out beyond the single cell, the shears may be found by extending the same principle. A detailed derivation for finding the redundant shears in a double torsion box is presented in appendix C.

In the type of section shown in figure 20 the shear in the extended flanges is statically determined because at the free edge the shear is known to be zero and the shear at any section of the extension may be obtained by the relation

$$q = \sum_0^n \frac{dP}{dy} \tag{12}$$

The shear from equation (12) can then be directly added to the shears in the box, and the problem is reduced to that of a single torque box.

Location of Shear Center

Once the shear stresses due to axial loads have been determined the shear center may be located. If the external shear loads are considered to act through the shear center, the moment of the shear stresses about any point such as the center of gravity must be equal to the moment of the shear loads about that point, for static equilibrium.

The moment of the shear flow q about the center of gravity is equal to q times twice the cross-hatched area in figure 21.

$$2dA = x_n z_{n+1} - x_{n+1} z_n$$

For a section of large curvature, such as in the nose D, the area between chord and curve may be estimated, doubled, and added to formula (13), if increased accuracy is desired.

Now resolve V_x and V_z into a single shear V and take moments

$$(V_x^2 + V_z^2)\, d = Vd = \Sigma q\ 2dA$$

$$d = \frac{\Sigma q\ 2dA}{V} \tag{14}$$

where d is the distance from the shear center to the center of gravity. Therefore,

$$\left.\begin{aligned} x_{s.c.} &= d\,\frac{V_z}{V} = \frac{V_z \Sigma q\ 2dA}{V^2} = \frac{V_z \Sigma q\ 2dA}{V_x^2 + V_z^2} \\ z_{s.c.} &= d\,\frac{V_x}{V} = \frac{V_x \Sigma q\ 2dA}{V^2} = \frac{V_x \Sigma q\ 2dA}{V_x^2 + V_z^2} \end{aligned}\right\} \tag{15}$$

The location of the shear center for each station should plot in a smooth spanwise curve if the original effectiveness curves are fairly accurate.

Shear Due to Torsion

Since V_x and V_z are not located at shear center, there will be a net torque on the section about the shear center.

$$T_{s.c.} = T_0 + V_z (x_{c.g.} + x_{s.c.}) - V_x (z_{c.g.} + z_{s.c.})$$

The shear flow q_t on any section due to this torque will be

$$q_t = \frac{T}{2A}$$

This shear flow can then be added to that due to the beam and the chord bending to give the total shear flow and hence the shear stress at any point.

Effect of Taper

Taper in both depth and width will affect the shear-stress distribution. Taper in width can usually be safely neglected. Taper in depth, however, is important in the design of the vertical webs, since the cap strips will carry a fair share of the applied shear load and relieve the vertical webs.

Consider the tapered panel in figure 22. Take moments about A and assume dy so small that V may be considered constant over its length.

$$V\,dy + Ph - dPh - Ph - Pdh = 0$$

$$V\,dy - dPh - Pdh = 0$$

$$V = \frac{dP}{dy} h + P \frac{dh}{dy} \qquad (16)$$

or, as expected, the applied shear is the sum of the web shear $\frac{dP}{dy} h$ and the shear carried by the cap strips $P \frac{dh}{dy}$. The slope between the cap strips is dh/dy. The web shear dP/dy has already been obtained entirely inde-

pendently of V by the methods outlined and equation (11) so that no taper correction will be necessary.

Equation (16) can be used, however, as a rough check on the shears obtained from equation (11) by computing the term $P \frac{dh}{dy}$ from the axial loads and slope, adding it to the vertical web shears, and checking the sum with V, the applied beam shear on the section.

Tabular Forms for Shear Computation

Table 3 has been developed for quick computation of shear stresses and shear center. A brief explanation is given here.

For ease in integration, elements should be numbered starting from the upper cap strip in a clockwise direction. Shear panels should be numbered in a clockwise direction corresponding to the adjacent counterclockwise element. Material in flanges extending beyond the torsion box should be numbered separately starting from the free edge. (See fig. 23.)

The cut will be taken in the vertical web, web A, with thickness t_a. Column 2 contains the width ds of each shear panel measured between elements. Columns 6 and 7 are the coordinates x and z of the various elements measured to the center of gravity of the section. These coordinates differ slightly from those of columns 12 and 13 of table 1 because in table 1 the coordinates are to the center of gravity of each element, while in table 3, the coordinates are measured to the point at which the element is attached to the skin. This method is necessary in order that the summation of moments will be accurate. These coordinates may be scaled off the rib drawings.

Columns 8 and 9 should be watched for signs and the absolute value of their algebraic difference should be entered in column 11. Column 10 need be used only where there is sharp curvature in the skin between elements, such as in the nose D. Columns 6 to 11 may be omitted if the shear-center calculation is neglected.

Columns 12, 13, and 14 give the rate of change of axial load for each element at the station in question. A tangent to the load curve is drawn at the station (see fig.

24) and the slope is computed. Column 15 is the progressive summation of the values in column 14 starting on the clockwise side of the cut vertical web. In column 17, q_b is the shear stress in any member due to bending only. (See equation (11).) From the shear-center location (calculated or estimated) and the computations in lines 3 to 9, the torsional shear q_t is obtained, which is added to q_b giving column 18. The right-hand term of equation (15) is obtained from the summation of column 19 and is used in the shear-center calculation in lines 12 and 13.

If it is desired to omit the shear-center calculation and solve for the shear stresses by the statically determinate method of references 7 and 10, the tabular form may still be used with slight modification. Columns 2 to 5 may be omitted. Columns 16, 24, and 30 should be changed to $\sum_B^N \frac{\Delta P}{\Delta y} \times 2\Delta A$, [column (15) x column (9)]. Columns 17 and 19 may be left out and a separate computation may be made for the correction shear at the cut section

$$\frac{V_B x_{c.g.} - V_C z_{c.g.} - \text{column (16)}}{2 \times \text{area of torque tube}} = q_{b+t}$$

which is then added to column (15) to get q in column (18).

Table 3 is worked out for station 232 of the wing for airplane B as an example. This section has projections beyond the torque box, which are handled as previously noted. Care must be taken that the proper sign is used for these projection shears. Note that the top-cover projection changes sign when added to the torque box in column (15).

For simplicity, the shear from element V is assumed to be divided evenly between top and bottom cover rather than computed as though it were a double torque box. Shears in the projections are unaffected by the torque shears on the box.

The load curve of figure 24 is a good check on the general trend of the stresses and the loads. Each stringer or cap strip should show a smooth curve. The slope of each curve at any point represents the load per inch that the rivets must transfer from skin to stringer. This fact can be used in designing the rivet spacing. The spacing

will be most critical where the curves are steepest, that is, at each end of the stringer.

The curves for J and G are caused by the reverse bending in the front beam, and the irregularities through the wheel-well region (station 142) are apparent in the cap strips B and N.

The values of $\Delta P/\Delta y$ of column 14 were obtained by drawing tangents to the load curves at station 232, reading values of P at station 222 and station 242, and dividing by $\Delta y = 20$. As a check on the accuracy of the calculations, the summation of column 14 should be approximately zero.

ANALYTICAL CHECK FOR EFFECTIVENESS CURVES

Final proof of the accuracy of the effectiveness curves and the axial and shear stresses obtained from them can be made by using the principle of consistent deformations.

In figure 25 assume that the applied loads cause the structure to deform as shown. If the effectiveness curves and the computed stresses are accurate, then the deformation of point H to H' should be the same, whether figured by the path A E' F' G' H' or by the path A B' C' D' H'. The first path will include axial deformation in AE plus shear deformations in panels EF, FG, and GH. The second path is made up of shear deformations in AB, BC, and CD, and axial deformation in DH.

Axial deformations will be computed by the formula

$$\partial_p = f_b \frac{\Delta y}{E}$$

where f_b is the average axial stress in a length Δy of a member. Shear deformation is computed from the relation

$$\partial_s = \frac{q\ ds}{t\ G_e}$$

The effective shear modulus G_e should be so selected that diagonal tension is considered.

In the following section a check is made for the wing of airplane B between stations 232 and 277. (See fig. 26.)

Calculations for shear stresses at station 277 are not included but are similar to those for station 232. For new work, approximate checks, which will serve as a very good control, can be made when the effectiveness curves are first drawn.

TOP COVER

In order to take diagonal tension into account from reference 2, G_e will be selected at $0.2G = 0.2 \times 4{,}000{,}000 = 800{,}000$ pounds per square inch.

SHEAR DEFORMATIONS

Panel	Station 232				Station 277			
	q (lb/in.)	t (in.)	ds (in.)	$\frac{qds}{tG_e}$	q (lb/in.)	t (in.)	ds (in.)	$\frac{qds}{tG_e}$
C	-4.9	0.040	7.40	-0.00113				
E	9.8	.040	11.20	.00343	-6.5	0.040	15.00	-0.00304
G	19.2	.040	12.00	.00720	2.0	.040	9.00	.00060
H	22.1	.040	7.00	.00483	19.5	.040	7.00	.00427
			Total	.01433 in.				.00183 in.

AXIAL DEFORMATION

Element	Average P (lb)	Average area (sq in.)	Δy (in.)	$\frac{P\Delta y}{AE}$
B	-1430	0.404	45	-0.01592
E	-510	.210	45	-.01092
G	-340	.204	45	-.00750
H	-65	.083	45	-.00352

Then from figure 26,

Path BB - BEGH $\quad 0.01592 + 0.00183 = 0.01775$ in.
Path BCEGH - HH $\quad 0.01433 + 0.00352 = 0.01785$ in.

This result checks very well, supporting the validity of the effectiveness curves. Such checks can be made wherever considered necessary.

Grumman Aircraft Engineering Corporation,
Bethpage, N. Y.

APPENDIX A

SIGN CONVENTIONS AND SYMBOLS

Signs

Applied loads:

Shear loads - positive up, rearward and outboard

Bending moments - positive if causing compression in upper rear corner of section

Pitching moments - positive if a stalling moment

Stresses:

Axial stresses - positive if tensile

Shear stresses - positive if in same direction as stalling moment (clockwise if section is viewed toward plane of symmetry of airplane)

Coordinates:

x, y, z - positive if rearward, outboard, and up from origin

Elemental skin widths, ds:

Integrations in clockwise direction (same direction as positive shear)

Symbols

The symbols used in this paper correspond to similar ones in references 1 and 11.

A cross-sectional area

A_F is flange, or cap-strip, area and includes any adjacent material considered to act with it. A_L is area of stringers from flange to center of panel and includes the effective adjacent sheet. If there is only one stringer, A_L is one-half the area of the stringer, $A_T = A_F + A_L$

P axial load

G shear modulus, including effect of tension fields

t thickness of cover sheet

E Young's modulus

b half-width of beam for single-stringer beams; distance from flange to center of gravity between flange and center line for a multistringer beam

K shear-lag parameter $\sqrt{\frac{Gt}{Eb}\left(\frac{1}{A_L}+\frac{1}{A_F}\right)}$

S shear force

h depth of beam

f stress

E' effectiveness factor (f_L/f_F)

E'_B and E'_C effectiveness factor for beam and chord bending

M bending moment (Ph)

I_{xx}, I_{zz}, I_{xz} geometric moments of inertia

γ shear strain

q running shear, pounds per inch of skin

F total change in length of flange

L length of panel from free end to plane of symmetry. Also total change in length of stringer

x distance along x axis measured from origin halfway between flanges of panel (equation (4)), or from reference point

z distance along z axis measured from reference point

$x_{s.c.}$, $y_{s.c.}$, $z_{s.c.}$ distance from center of gravity of material to shear center

$x_{c.g.}$, $y_{c.g.}$, $z_{c.g.}$ distance from load axis to c.g. of section

Y	auxiliary parameter
α	angle of attack
W	total work
T	torque
V	applied shear on the section
V_x, V_z	applied beam chord shear on section
ds	width of shear panel
∂_p	axial deformation
∂_s	shear deformation

Subscripts

t	due to torque
b	due to bending
a	at section a
e	effective
B	beam
c	chord
F	flange
L	stringer
s	shear
T	total
W	web
C	cover sheet
c.g.	center of gravity
s.c.	shear center
n	at section n
0	origin

APPENDIX B

DETAILED DERIVATION OF SPANWISE EFFECTIVENESS EQUATION

The fundamental equations are:

$$dP_L = dS_L \tag{1a}$$

$$dP_F = \frac{S_W\, dy}{h} - dS_C \tag{1b}$$

$$df_s = \frac{-G}{Eb}\,(f_F - f_L)\,dy \tag{1c}$$

In equation (1a)

$$dP_L = df_L A_L \qquad dS_C = f_s t dy \tag{a}$$

so that if equation (1a) is differentiated and equation (1c) is substituted,

$$\frac{d^2 f_L}{dy^2} = \frac{df_s}{dy}\,\frac{t}{A_L} = -\frac{Gt}{EbA_L}\,(f_F - f_L) \tag{b}$$

From equations (1a) and (a)

$$f_L = \int \frac{f_s t}{A_L}\,dy \tag{c}$$

From equations (1b) and (a)

$$f_F = \int \frac{S_W dy}{A_F h} = \int \frac{f_s t}{A_F}\,dy \tag{d}$$

and from equations (c) and (d)

$$f_F = \int \frac{S_W dy}{A_F h} - \frac{A_L}{A_F}\,f_L \tag{e}$$

Substitute equation (e) in equation (b) and simplify

$$\frac{d^2f_L}{dy^2} = \frac{Gt}{Eb}\left(\frac{1}{A_L} + \frac{1}{A_F}\right) f_L - \frac{Gt}{EbA_L}\int \frac{S_W dy}{A_f h}$$

$$= \frac{Gt}{Eb}\left(\frac{1}{A_L} + \frac{1}{A_F}\right) f_L - \frac{Gt}{Eb}\,\frac{1}{A_L A_F}\,\frac{A_L + A_F}{A_L + A_F}\int \frac{S_W dy}{h}$$

Since

$$\frac{A_L + A_F}{A_L A_F} = \frac{1}{A_L} + \frac{1}{A_F}$$

and

$$A_L + A_F = A_T$$

$$\frac{d^2f_L}{dx^2} = \frac{Gt}{Eb}\left(\frac{1}{A_L} + \frac{1}{A_F}\right)\left(f_L - \int \frac{S_W dy}{A_T h}\right) \qquad (f)$$

Let

$$K^2 = \frac{Gt}{Eb}\left(\frac{1}{A_L} + \frac{1}{A_F}\right)$$

Also $S_W dy = dM$, so that equation (f) becomes

$$\frac{d^2f_L}{dy^2} - K^2 f_L + K^2 \frac{M}{A_T h} = 0 \qquad (g)$$

and by analogous derivations,

$$\frac{d^2f_F}{dy^2} - K^2 f_F + K^2 \frac{M}{A_T h} = 0 \qquad (h)$$

$$\frac{d^2f_s}{dy^2} - K^2 f_s + K^2 \frac{S_W AL}{htA_T} = 0 \qquad (i)$$

In the NACA methods of analysis, equations (g), (h), and (i) are solved by means of arithmetic integration so that if K, M, S_W, h, t, A_L, A_F, and b are variable along the span, they may be taken into consideration. (See references 1 to 6.)

The solution of equations (g), (h), and (i) will be

obtained for the following conditions:

$$K^2 = \text{a constant}$$

$$\frac{M}{hA_T} = \text{a constant } D$$

$$\frac{S_W A_L}{htA_T} = \text{a constant } R$$

Let p denote the operation d/dy; then equation (g) becomes

$$(p^2 - K^2)\, f_L = - K^2 \frac{M}{hA_T}$$

Take the first derivative to eliminate the constant

$$p\,(p^2 - K^2)\, f_L = 0 \qquad (j)$$

This is a linear differential equation that has a solution in the form

$$f_L = Ae^{m_1 y} + Be^{m_2 y} + Ce^{m_3 y} \qquad (k)$$

where m_1, m_2, and m_3 are the roots of equation (j) for m substituted for p and f_L = unity.

$$m(m^2 - K^2) = 0$$

or

$$m_1 = -K \qquad m_2 = K \qquad m_3 = 0$$

or equation (k) becomes

$$f_L = Ae^{-Ky} + Be^{Ky} + C \qquad (l)$$

If equation (l) is substituted in equation (g) and is then solved for C, it will be seen that

$$C = \frac{M}{hA_T} = D$$

Thus the solution of equation (g) for the condition stated is

$$f_L = Ae^{-Ky} + Be^{Ky} + D \qquad (m_1)$$

Similarly

$$f_F = Ee^{-Ky} + Fe^{Ky} + D \qquad (m_2)$$

$$f_s = Ne^{-Ky} + Qe^{Ky} + R \qquad (m_3)$$

Coefficients A, B, E, F, N, and Q are determined by the boundary conditions for the particular problem considered.

Stringer stress.- For the beam of figure 3 the following boundary conditions hold when

$$y = 0 \qquad f_L = 0$$

and when

$$y = L \qquad \frac{df_L}{dy} = 0$$

Substitute in equation (m_1)

$$A + B + D = 0$$

$$-KAe^{-KL} + KBe^{KL} = 0$$

Solve simultaneously for A and B

$$A = \frac{-De^{KL}}{2 \cosh KL}$$

$$B = \frac{-De^{-KL}}{2 \cosh KL}$$

Substitute in (m_1) and simplify

$$f_L = \frac{D}{2 \cosh KL}\left[-e^{K(L-y)} - e^{-K(L-y)}\right] + D$$

$$f_L = D\left[1 - \frac{\cosh K(L-y)}{\cosh KL}\right] \qquad (2b)$$

Cap-strip stress.- The boundary conditions for the cap strip are:

When

$$y = 0$$

$$f_F = \frac{M}{A_F h}$$

and when

$$y = L$$

$$\frac{df_F}{dy} = 0$$

In a manner similar to the stringers,

$$f_F = D\left[1 + \frac{A_L}{A_F}\frac{\cosh K(L-y)}{\cosh KL}\right] \qquad (2a)$$

APPENDIX C

DERIVATION OF EQUATIONS FOR BEAM SHEAR IN DOUBLE-CELL TORQUE BOXES

In terms of the shears (see fig. 27) at the cut sections q_1 and q_2, the variable shears in the three parts of the loop q_b, q_c, and q_d are

$$q_b = q_1 - \sum_1^b \frac{dP}{dy} \qquad f_{s_b}t = f_{s_1}t_1 - \sum_1^b \frac{dP}{dy}$$

$$q_c = q_1 - q_2 + \sum_{1,2}^c \frac{dP}{dy} \qquad f_{s_c}t = f_{s_1}t_1 - f_{s_2}t_2 + \sum_{1,2}^c \frac{dP}{dy} \qquad (a)$$

$$q_d = q_2 + \sum_2^d \frac{dP}{dy} \qquad f_{s_d}t = f_{s_2}t_2 + \sum_2^d \frac{dP}{dy}$$

In order to find the values of q_1 and q_2, the least-work solution is applied (see reference 12) to the two loops (1) and (2):

$$W_1 = \frac{1}{2G}\int_c^b f_{s_b}^2 t\,ds + \frac{1}{2G}\int_a^c f_{s_c}^2 t\,ds \qquad (b_1)$$

$$W_2 = \frac{1}{2G}\int_a^c f_{s_d}^2 t\,ds + \frac{1}{2G}\int_a^c f_{s_c}^2 t\,ds \qquad (b_2)$$

Perform the operations

$$\frac{\partial W_1}{\partial f_{s_1}} = 0 \qquad \frac{\partial W_2}{\partial f_{s_2}} = 0$$

and equations (b_1) and (b_2) become

$$\int_c^a f_{s_b}\, t\, \frac{\partial f_{s_b}}{\partial f_{s_1}}\, ds + \int_a^c f_{s_c}\, t\, \frac{\partial f_{s_c}}{\partial f_{s_1}}\, ds = 0 \qquad (c_1)$$

$$\int_a^c f_{s_d}\, t\, \frac{\partial f_{s_d}}{\partial f_{s_2}}\, ds + \int_a^c f_{s_c}\, t\, \frac{\partial f_{s_c}}{\partial f_{s_2}}\, ds = 0 \qquad (c_2)$$

But

$$\frac{\partial f_{s_b}}{\partial f_{s_1}} = \frac{t_1}{t}, \quad \frac{\partial f_{s_c}}{\partial f_{s_1}} = \frac{t_1}{t}, \quad \frac{\partial f_{s_c}}{\partial f_{s_2}} = \frac{-t_2}{t}, \quad \frac{\partial f_{s_d}}{\partial f_{s_2}} = \frac{t_2}{t}$$

Substitute these expressions in equations (c_1) and (c_2) and simplify

$$\int_c^a f_{s_b} t_1\, ds + \int_a^c f_{s_c} t_1\, ds = 0 \qquad (d_1)$$

$$\int_a^c f_{s_d} t_2\, ds - \int_a^c f_{s_c} t_2\, ds = 0 \qquad (d_2)$$

Substitute equations (a) in equations (d_1) and (d_2)

$$\int_c^a \frac{t_1}{t}\, q_1\, ds - \int_c^a \frac{t_1}{t}\, ds \sum_1^b \frac{dP}{dy} + \int_a^c \frac{t_1}{t}\, q_1\, ds - \int_a^c \frac{t_1}{t}\, q_2\, ds$$

$$+ \int_a^c \frac{t_1}{t}\, ds \sum_{1,2}^c \frac{dP}{dy} = 0$$

$$\int_a^c \frac{t_2}{t} q_2 ds + \int_a^c \frac{t_2}{t} ds \sum_2^d \frac{dP}{dy} - \int_a^c \frac{t_2}{t} q_1 ds - \int_a^c \frac{t_2}{t} q_2 ds$$

$$- \int_a^c \frac{t_2}{t} ds \sum_{1,2}^c \frac{dP}{dy} = 0$$

Simplify

$$q_1 \int_c^a \frac{t_1}{t} ds - q_2 \int_a^c \frac{t_1}{t} ds = \int_c^a \frac{t_1}{t} ds \sum_1^b \frac{dP}{dy}$$

$$- \int_a^c \frac{t_1}{t} ds \sum_{1,2}^c \frac{dP}{dy} \qquad (e_1)$$

$$q_2 \int_d^a \frac{t_2}{t} ds - q_1 \int_a^c \frac{t_2}{t} ds = \int_a^c \frac{t_2}{t} ds \sum_{1,2}^c \frac{dP}{dy}$$

$$- \int_a^c \frac{t_2}{t} ds \sum_2^d \frac{dP}{dy} \qquad (e_2)$$

Equations (e_1) and (e_2), although apparently complicated, are easily obtainable in a tabular computation by progressive summation. Values of q_1 and q_2 can be solved for simultaneously and substituted in equations (a) for the shears at any section.

In the integration $\sum_{1,2}^c \frac{dP}{dy}$ for the common web, both upper and lower cap strips should be involved, while in the other integration they should be omitted. Skin effective in bending may be included in an approximate manner by considering the area concentrated at the center of the panel and then treating it as an extra stringer.

Triple torque boxes may also be handled by a similar derivation, there being three equations such as equations (e_1) and (e_2) to solve simultaneously.

The shear center may be found in the same manner as

for a single torque box as soon as the bending shears are determined, by taking a moment of these shears about the center of gravity and equating it to the moment of the external shears about the center of gravity.

REFERENCES

1. Kuhn, Paul, and Chiarito, Patrick T.: Shear Lag in Box Beams - Methods of Analysis and Experimental Investigation. NACA A.R.R., May 1941.

2. Kuhn, Paul: Stress Analysis of Beams with Shear Deformation of the Flanges. Rep. No. 608, NACA, 1937.

3. Kuhn, Paul: Approximate Stress Analysis of Multi-stringer Beams with Shear Deformation of the Flanges. Rep. No. 636, NACA, 1938.

4. Kuhn, Paul: Some Notes on the Numerical Solution of Shear-Lag and Mathematically Related Problems. T.N. No. 704, NACA, 1939.

5. Kuhn, Paul: A Recurrence Formula for Shear-Lag Problems. T.N. No. 739, NACA, 1939.

6. Newell, Joseph H.: The Analysis of Leading-Edge Wing Beams. SAE Jour., vol. 45, no. 3, Sept. 1939, pp. 285-288.

7. Shanley, F. R., and Cozzone, F. P.: Unit Method of Beam Analysis. Jour. Aero. Sci., vol. 8, no. 6, April 1941, pp. 246-255.

8. Sibert, H. W.: Shear Distribution in a Sheet-Metal Box Spar. Jour. Aero. Sci., vol. 5, no. 4, Feb. 1938, pp. 134-137.

9. Hatcher, R. S.: Rational Shear Analysis of Box Girders. Jour. Aero. Sci., vol. 4, no. 6, April 1937, pp. 233-238.

10. Hatcher, R. S.: Letter to the Editor. Jour. Aero. Sci., vol. 5, no. 9, July 1938, pp. 368-369.

11. Anon.: Strength of Aircraft Elements. ANC-5, Army-Navy-Civil Committee on Aircraft Requirements. U. S. Govt. Printing Office, 1940.

12. Sibert, H. W.: Shear Center of a Multi-Cell Metal Wing. Jour. Aero. Sci., vol. 8, no. 4, Feb. 1941, pp. 162-166.

TABLE I - SECTION PROPERTIES AT STATION _____

1	2	3	4	5	6	7	8	9	10	11	12	13	14	15	16	17
Element	Components of Element	Area A	Effectiveness Factor E'	E'A	x_o +	z_o +	$E'Ax_o$	$E'Az_o$	$E'Ax_o^2$	$E'Zx_o^2$	Positive Lift: Distance to C.G. $\bar{x}$ =	Positive Lift: Distance to C.G. $\bar{z}$ =	Positive Lift: I_{xz} E'Axz	Negative Lift: Distance to C.G. $\bar{x}$ =	Negative Lift: Distance to C.G. $\bar{z}$ =	Negative Lift: I_{xz} E'Axz
		$\sum(2)$		(3)x(4)			(5)x(7)	(5)x(6)	(7)x(8)	(6)x(9)	(6)-$\bar{x}$	(7)-$\bar{z}$	(8)x(12) x(13)	(6)-$\bar{x}$	(7)-$\bar{z}$	(5)x(15) x(16)
	SUB TOTALS															
	POSITIVE LIFT TOTALS				$\bar{x}$=	$\bar{z}$=										
	NEGATIVE LIFT TOTALS				$\bar{x}$	$\bar{z}$										
	CHECKS										(a)	(a)		(a)	(a)	

STATION

18	19	20	21	22	23	24	25	26	27
	Condition	M_B	M_C	C_2M_B	C_3M_B	C_2M_C	C_4M_B	K_1	K_2
		x10^6	x10^6	C_2(20)	C_3 (21)	C_2(21)	C_4(20)	(22)-(23)	(24)-(25)
POSITIVE LIFT									
NEGATIVE LIFT									

VALUES OF I_{xx}, I_{zz}, AND I_{xz}

	Positive Lift	Negative Lift
$I_{xz} = \sum(14)$ or $\sum(17)$		
$I_{xx} = \sum(10) - \bar{z}^2 \sum(5)$	+	+
$I_{zz} = \sum(11) - \bar{x}^2 \sum(5)$	+	+
$I_{xx} I_{zz} - K^2$	+	+

VALUES OF BENDING CONSTANTS

	Positive Lift	Negative Lift
$C_1 = \frac{10^6}{I_{xx}I_{zz}-K^2}$	+	+
$C_2 = KC_1$		
$C_3 = I_{xx}C_1$	+	+
$C_4 = I_{zz}C_1$	+	+

Notes:

(a) Arithmetic check: For (12)(13)(15)&(16) and N
Items (6) = (12)+N$\bar{x}$ = (15)+N$\bar{x}$, (7)= (13)+N$\bar{z}$= (16)+N$\bar{z}$

TABLE II - 10 BENDING STRESSES AND AXIAL LOADS AT STATION ________

STATION

1	2	3	4	5	6	7	8	9	10	11	12	13	14	15	16	17	18	19	20	21	22	23	24	25	26	27	28	29	30	31
Element N	Area A	Effectiveness Factor	Direction of Lift	x	z	Operation in Col(8) (11)(14) (17) Etc.	POSITIVE LIFT												ZERO LIFT			NEGATIVE LIFT								
							α = +			α = +			α = +			α = +			α =			α = -			α = -			α = -		
							Δf_b	f_b	P	Δf_b	f_b	P	Δf_b	f_b	P	Δf_b	f_b	P	Δf_b	f_b	P	Δf_b	f_b	P	Δf_b	f_b	P	Δf_b	f_b	P
$(1)_1$	$(3)_1$	$(4)_1$		$(12)_1 \div (15)_1$	$(13)_1 \div (16)_1$	$K_1=(26)_1$ $K_2=(27)_1$	(7)	Σ(8)	(2)x(9)	(7)	Σ(11)	(2)x(12)	(7)	Σ(14)	(2)x(15)	(7)	Σ(17)	(2)x(18)	(7)	Σ(20)	(2)x(21)	(7)	Σ(23)	(2)x(24)	(7)	Σ(26)	(2)x(27)	(7)	Σ(29)	(2)x(30)
			+			$K_1 x E'$																								
			-			$K_2 x E'$																								
			+			$K_1 x E'$																								
			-			$K_2 x E'$																								
			+			$K_1 x E'$																								
			-			$K_2 x E'$																								
			+			$K_1 x E'$																								
			-			$K_2 x E'$																								
			+			$K_1 x E'$																								
			-			$K_2 x E'$																								
			+			$K_1 x E'$																								
			-			$K_2 x E'$																								
			+			$K_1 x E'$																								
			-			$K_2 x E'$																								
			+			$K_1 x E'$																								
			-			$K_2 x E'$																								
			+			$K_1 x E'$																								
			-			$K_2 x E'$																								
			+			$K_1 x E'$																								
			-			$K_2 x E'$																								
			+			$K_1 x E'$																								
			-			$K_2 x E'$																								
			+			$K_1 x E'$																								
			-			$K_2 x E'$																								
			+			$K_1 x E'$																								
			-			$K_2 x E'$																								
			+			$K_1 x E'$																								
			-			$K_2 x E'$																								
			+			$K_1 x E'$																								
			-			$K_2 x E'$																								
			+			$K_1 x E'$																								
			-			$K_2 x E'$																								
			+			$K_1 x E'$																								
			-			$K_2 x E'$																								
			+			$K_1 x E'$																								
			-			$K_2 x E'$																								
			+			$K_1 x E'$																								
			-			$K_2 x E'$																								
			+			$K_1 x E'$																								
			-			$K_2 x E'$																								
			+			$K_1 x E'$																								
			-			$K_2 x E'$																								
			+			$K_1 x E'$																								
			-			$K_2 x E'$																								
			+			$K_1 x E'$																								
			-			$K_2 x E'$																								

TABLE XII - SHEAR CENTER AND 1G RUNNING SHEAR AT STATION 232 FOR AIRPLANE-B WING.

	SHEAR CONSTANTS				SHEAR CENTER CONSTANTS						POSITIVE LIFT				α = +16°				α =					
1	2	3	4	5	6	7	8	9	10	11	12	13	14	15	16	17	18	19	20	21	22	23	24	25
Element or Web	ds	t	$\frac{t_a}{t}$ t_a=.064	$\frac{t_a}{t}$ ds	x	z	$x_{n+1}z_n$	$x_n z_{n+1}$	Area Between Chord & Web	2ΔA From C.G. All Plus	Axial Load at Sta. 242	Axial Load at Sta. 222	$\frac{\Delta P}{\Delta y}$ Δy = 20	Progressive sum of $\frac{\Delta P}{\Delta y}$	$\sum_b^n \frac{\Delta P}{\Delta y}$ x $\frac{t_a}{t}$ ds	q_b= (16)-q_a+	q q_a + q_t	q_bx2ΔA	Axial Load at Station	Axial Load at Inboard Sta.	$\frac{\Delta P}{\Delta Y}$ ΔY =	Progress. Sum Of $\frac{\Delta P}{\Delta Y}$	$\sum_B^N \frac{P}{Y}$ x $\frac{t_a}{t}$ ds	q =(23)+ q_t - q_a
			(3)	(2)x(4)	$(12)_1$	$(13)_1$	$\frac{(6)_{n+1}}{(7)_n}$ x	$\frac{(6)_n}{(7)_{n+1}}$ x		(8)-(9) +(10)	P	P_{in}	(15)-(12) Δy	$\sum_b^n \frac{\Delta P}{\Delta y}$	(15)x(5)	q_a= 2 = 49.3	q_t=7.0	(17)x(11)	P P_g	P_{in} P_{g_o}	(21)-(20) Y	$\sum_B^N \frac{\Delta P}{\Delta Y}$	(23)x(5)	q_t - q_a =
B	11.80	.064	1.0													-49.3	-42.3							
N	8.00	.040	1.6	12.80	4.6	-4.1	13.9	- 18.4		32.3	1094	1630	26.8	36.6	468	-12.7	- 5.7	-416						
R	5.70	.040	1.6	9.11	- 3.4	-4.0	36.4	12.9		23.5	1222	1400	17.0	53.6	489	4.3	11.3	101						
L	5.60	.040	1.6	8.96	- 9.1	-3.8	55.8	30.0		25.8	299	352	5.6	59.2	531	9.9	16.9	255						
Q	5.50	.040	1.6	8.80	-14.7	-3.5	66.4	38.2		28.2	242	335	4.5	63.7	561	14.4	21.4	406						
J	6.30	.040	1.6	10.10	-20.1	-2.6	65.0	8.0	2.7	59.7	18	33	1.2	64.9	664	18.6	22.6	933						
H	7.00	.040	1.6	11.20	-25.0	- .4	8.2	- 97.5	3.1	106.8	- 74	- 84	- 0.5	64.4	721	15.1	22.1	1642						
G	12.00	.040	1.6	19.20	-20.4	3.8	-36.1	-140.8		104.7	- 446	- 504	- 2.9	61.5	1181	12.2	19.2	1290						
E	11.20	.040	1.6	17.90	- 9.0	6.9	15.2	- 60.2		75.4	- 569	- 778	- 9.4	52.1	933	2.8	9.8	211						
C	7.40	.040	1.6	11.80	2.2	6.7	63.6	15.9		49.7	- 680	- 886	-14.7	37.4	441	-11.9	- 4.9	- 501						
B	11.80	.064	1.0	11.80	9.5	6.3	29.0	- 38.0		66.0	-1860	-2500	-37.0	.4	5	-49.3	-42.3	-3353						
				121.37						577.1			- 9.4		5984									
W		.020			19.0	0	0	108.2		108.2	20	33	0.7	- .7		- .7	- .7	- 76						
A		.020			17.3	5.7	109.0	54.1		54.9	- 26	- 48	- 1.1	.4		.4	.4	22						
													- .4											
V		.020			19.0	0	0	- 72.1		72.1	20	33	.7	.7		.7	.7	50						
U		.020			15.4	-3.8	-38.7	- 61.6		25.9	12	22	.5	1.2		1.2	1.2	31						
T		.020			9.4	-4.0	-27.6	- 36.5		10.9	48	80	.7	1.9		1.9	1.9	21						
S		.040			6.9	-4.1	-15.9	- 26.3		9.4	420	578	7.9	9.8		9.8	9.8	92						
													9.8											
												Total	0.0											
													(a)	(a)							(a)	(a)		

ROW	ITEM	REFERENCE	CONDITION α = +16°	α =	α =
1	q_a-Shear at Cut Web	Σ(16)+Σ(5)	49.3		
2	Beam Shear - V_B	Pg. II-45	960		
3	Chord Shear - V_C	Pg. II-46	-155		
4	$V_B^2 + V_C^2$	[2]^2 + [3]^2	945500		
5	Torsion-at Load Axis	Pg. IV-8	7500		
6	$V_B(X_{c.g.}+X_{s.c.})$	[3] x [16]	-6570		
7	$V_C(Z_{c.g.}+Z_{s.c.})$	[4] x [17]	-3350		
8	T_{sc}=[5] + [6] - [7]		4280		
9	$q_t = T_{sc}/2A$	[8] ÷ [11]	7		
10	$q_t = q_a$	[9] - [1]			

ROW	SHEAR CENTER CALCULATION ITEM		REFERENCE	VALUE
11	2xArea of Torque Tube			610.6
12	C. G. to Shear Center	$X_{s.c.}$+	$\Sigma(19)\frac{2}{A}$	- 0.62
13		$Z_{s.c.}$+	$\Sigma(19)\frac{2}{A}$	- 0.10
14	Load Axis to C.G.	$X_{c.g.}$+	Pg. IV-8	- 6.23
15		$Z_{c.g.}$+	Pg. IV-8	+21.7
16	$X_{s.c.}+X_{c.g.}$		[12] + [14]	- 6.85
17	$Z_{s.c.}+Z_{s.c.}$		[13] + [14]	21.60
18				
19				

Note-(a) $\Sigma P = P_{in} = \frac{\Delta P}{\Delta y} = 0$

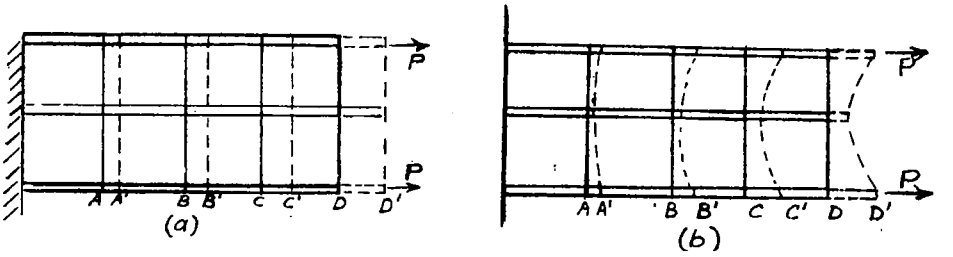

Figure 1.

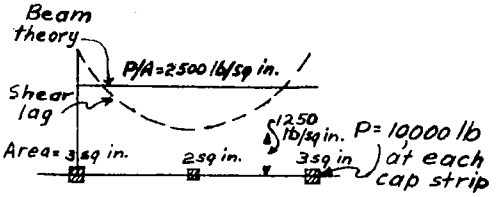

Figure 2.

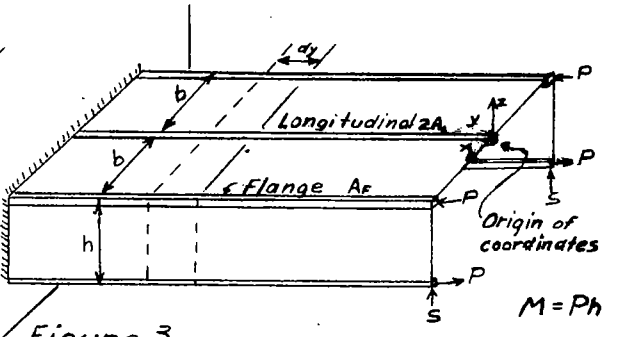

Figure 3.

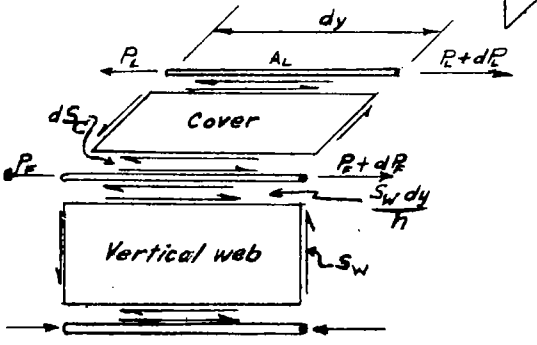

Figure 4.- Free-body diagram to show internal as well as external forces acting on each element.

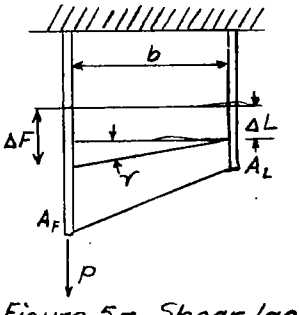

Figure 5.- Shear lag in single cover sheet. Shear strain, $\gamma = \frac{\Delta F - \Delta L}{b}$.

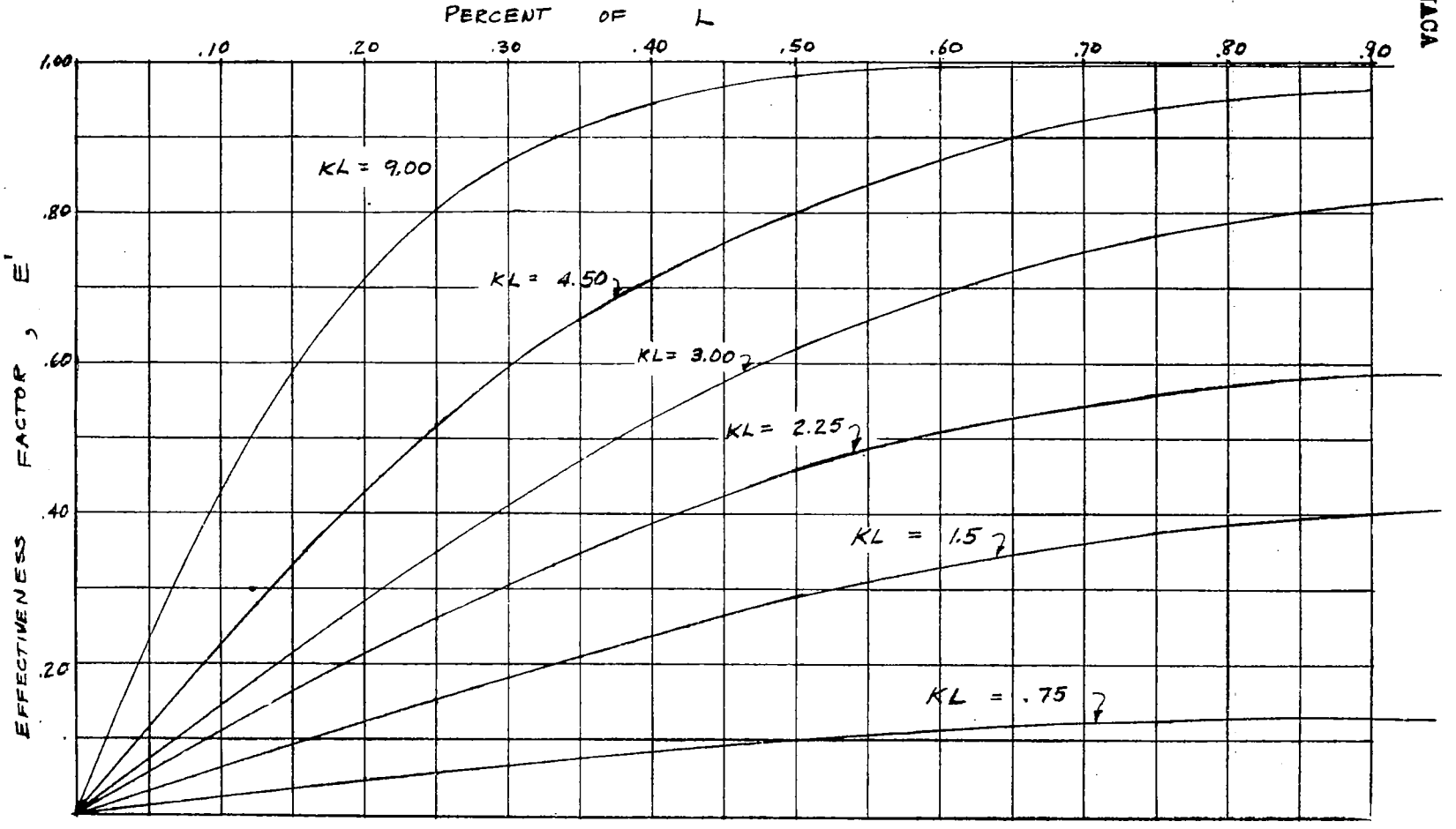

FIGURE 6.— IDEAL SPANWISE EFFECTIVENESS CURVES FOR SINGLE-STRINGER, CONSTANT-SECTION BOX BEAMS. $A_L/A_F = 1.00$

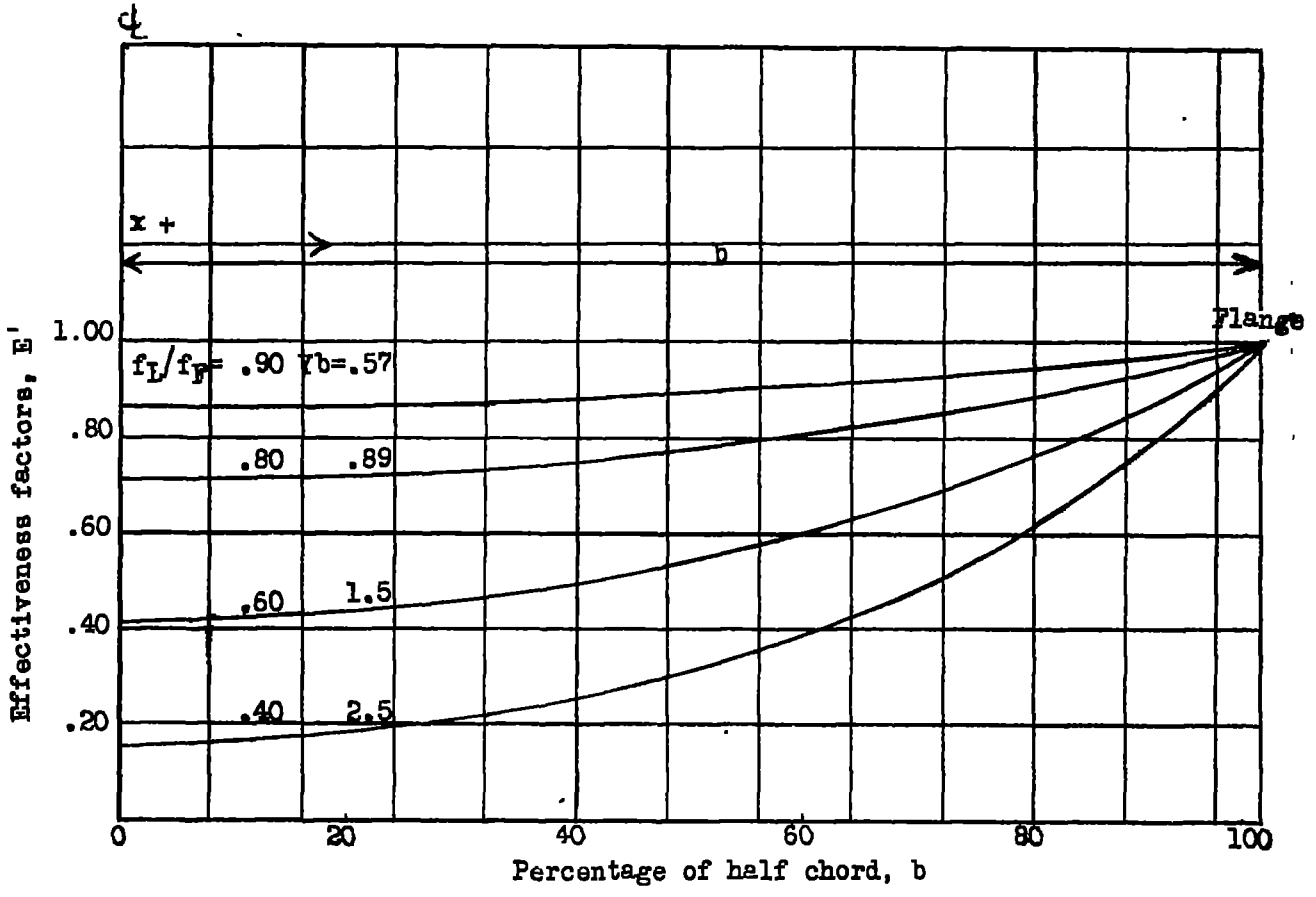

Figure 7.- Ideal chordwise effectiveness curves for continuous cover sheet or an infinite number of stringers.

$$E' = \frac{\cosh(Yb \cdot \frac{x}{b})}{\cosh Yb} \quad \text{where} \quad \frac{\tanh Yb}{Yb} = f_L/f_F.$$

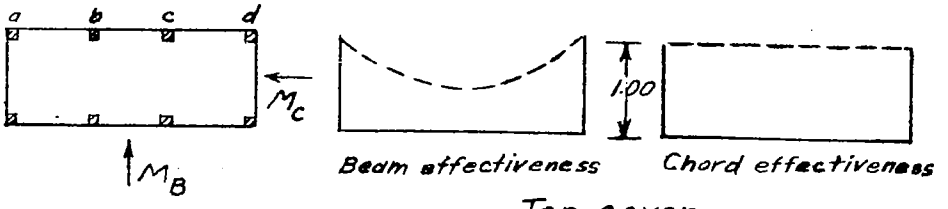

Figure 8.

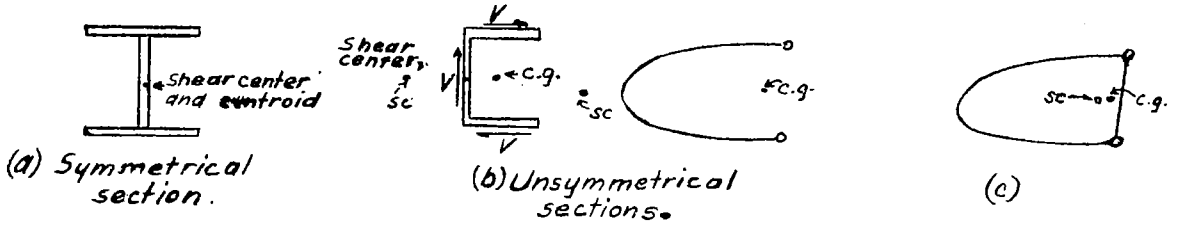

Figure 9.

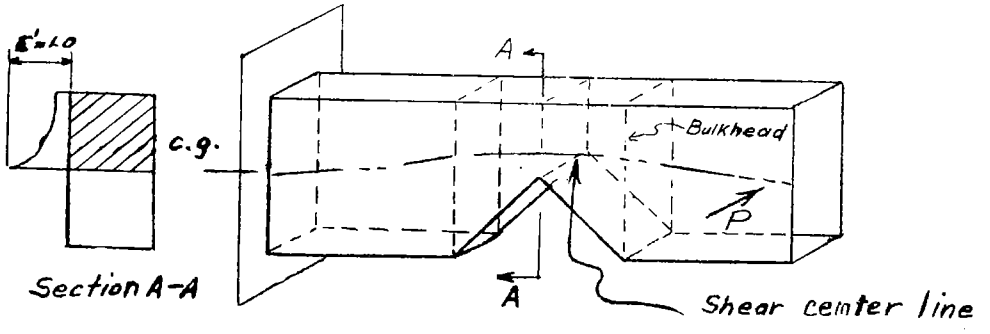

Figure 10.

NACA

Fig 11

PLAN FORM AND TYPICAL CROSS SECTION OF WING FOR AIRPLANE A

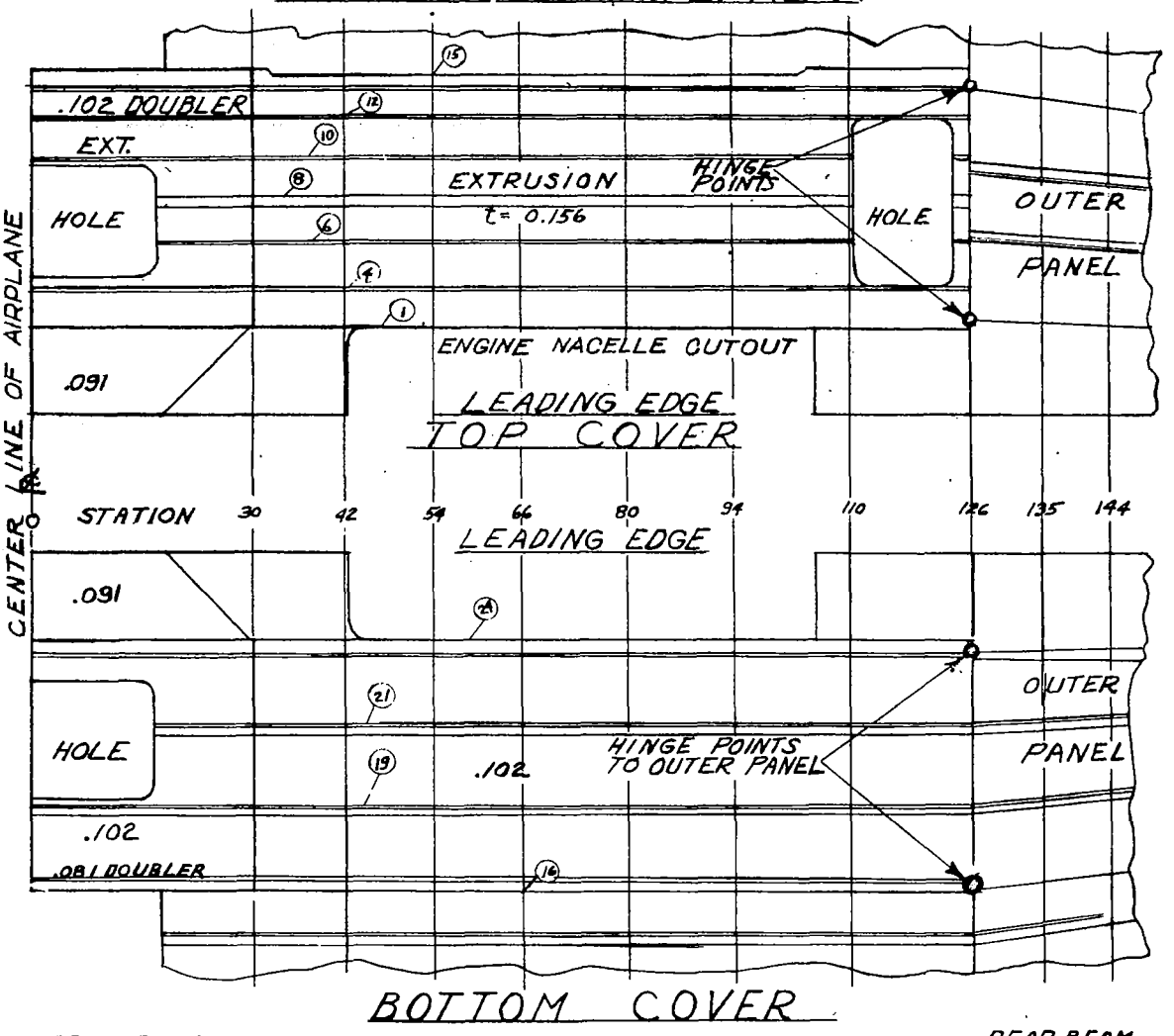

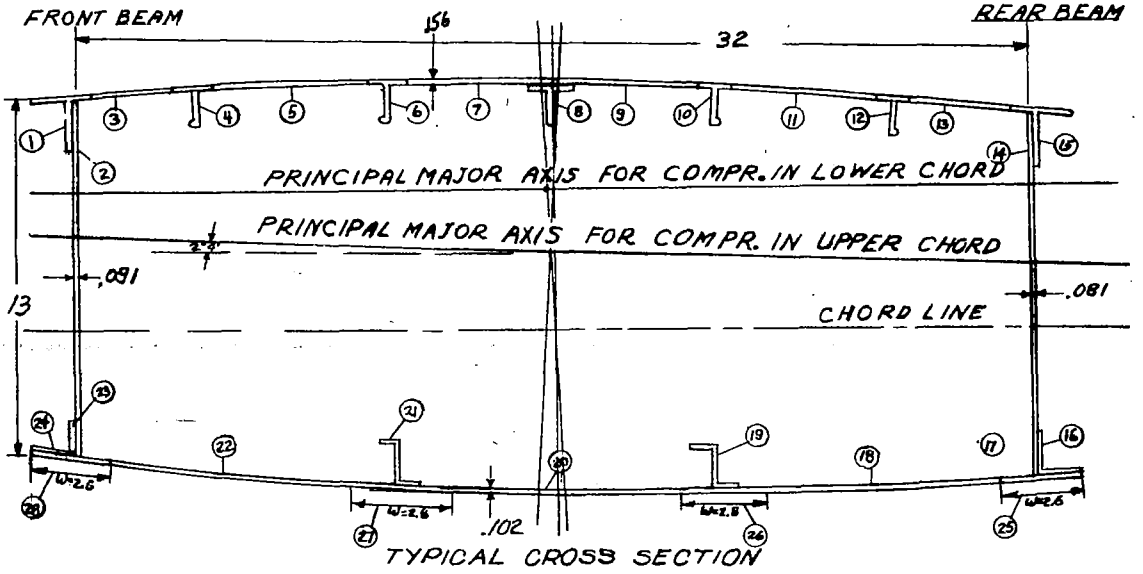

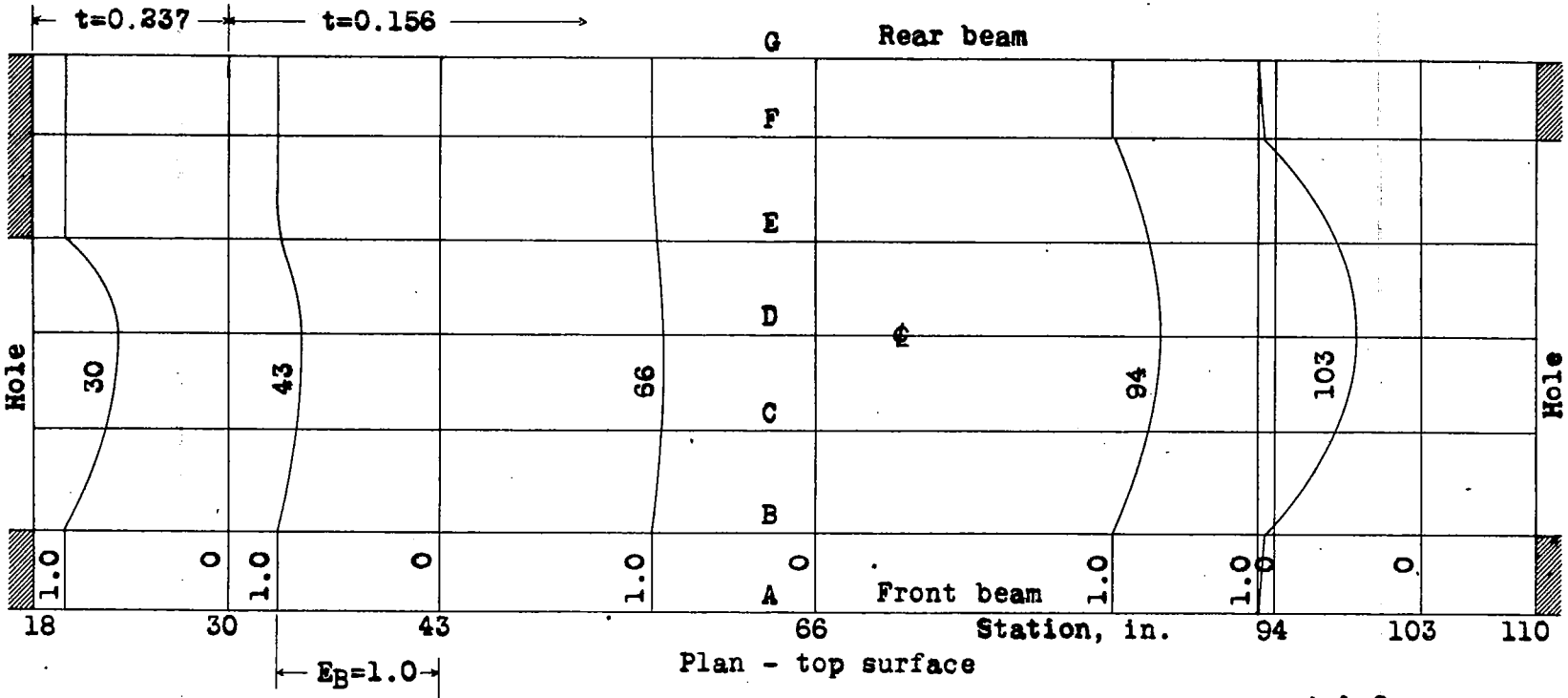

Plan - top surface

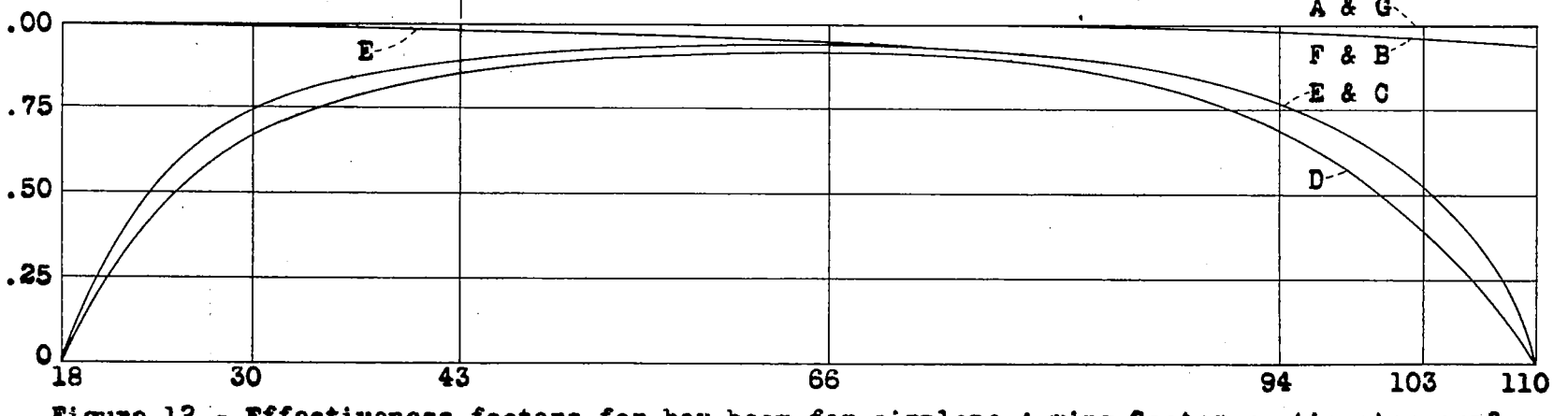

Figure 12.- Effectiveness factors for box beam for airplane-A wing. Center section; top surface.

NACA

Fig. 12

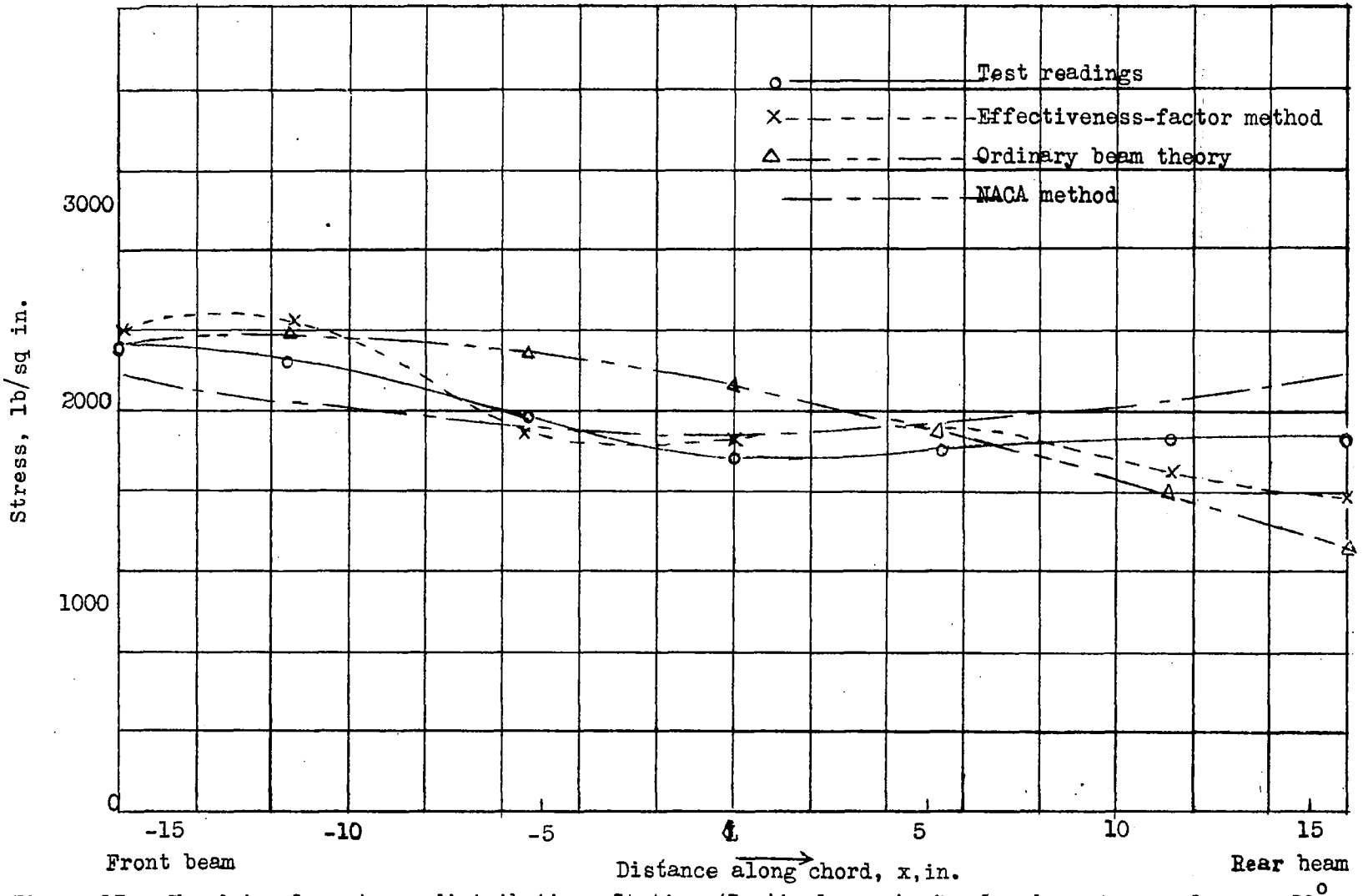

Figure 13,- Chordwise 1 g stress distribution. Station 43, Airplane—A wing box beam; top surface; $\alpha=20^{\circ}$. NACA method is for beam bending only. Chord bending would raise front-beam stress and lower rear-beam stress without changing curve shape and would improve agreement.

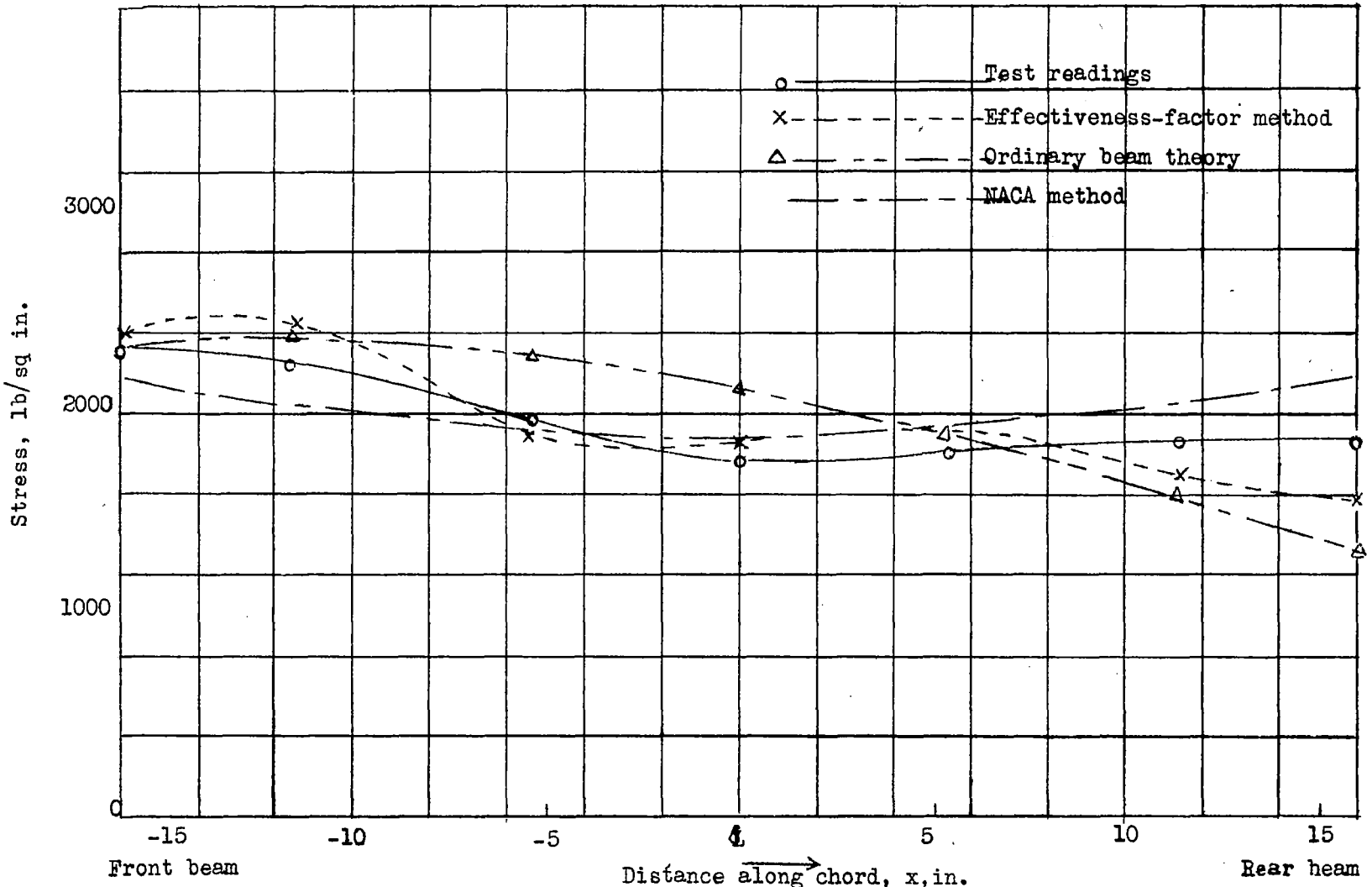

Figure 13,- Chordwise 1 g stress distribution. Station 43, Airplane—A wing box beam; top surface; $\alpha=20^{\circ}$. NACA method is for beam bending only. Chord bending would raise front-beam stress and lower rear-beam stress without changing curve shape and would improve agreement.

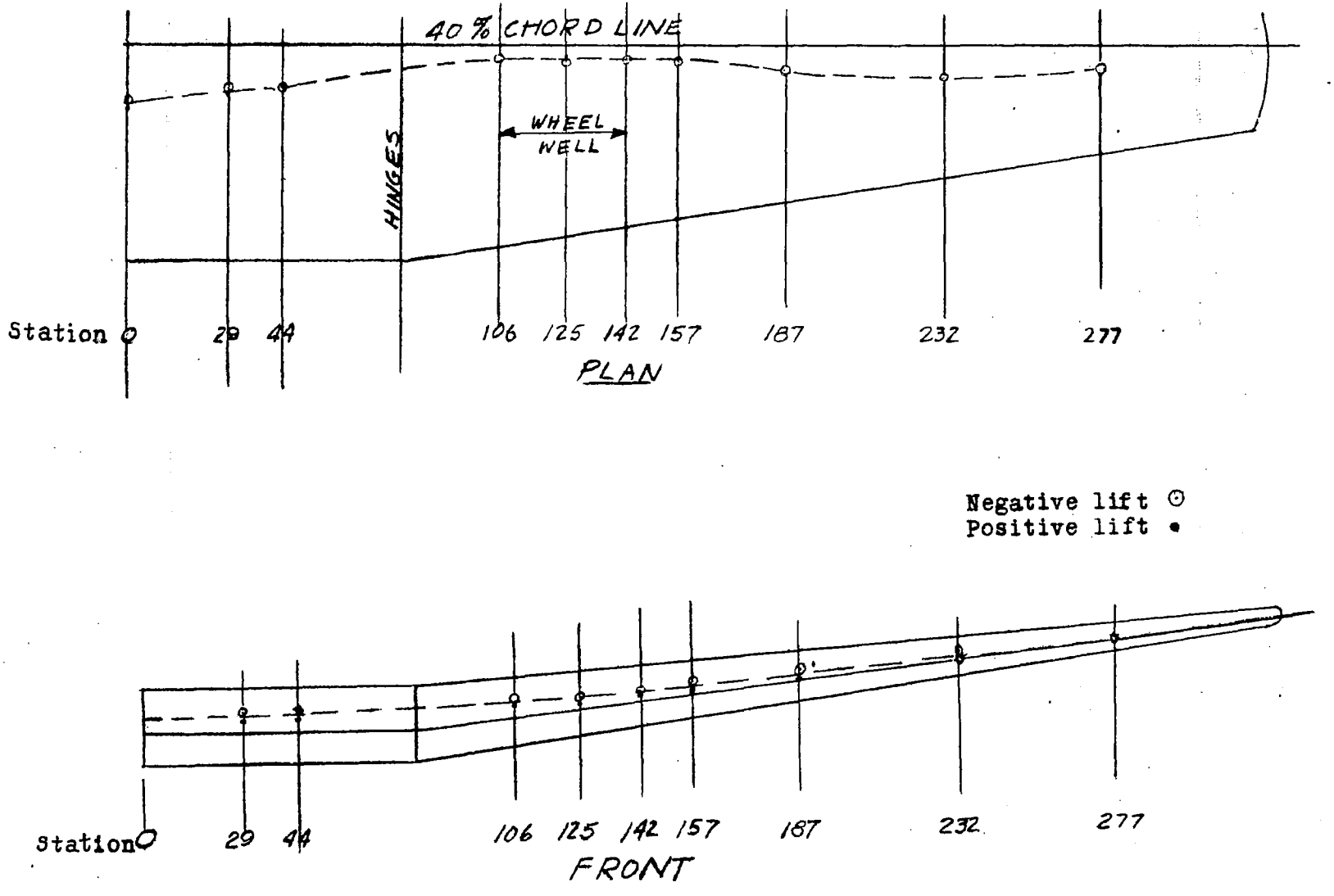

Figure 14.- Location of center of gravity of effective bending material for wing of airplane-B.

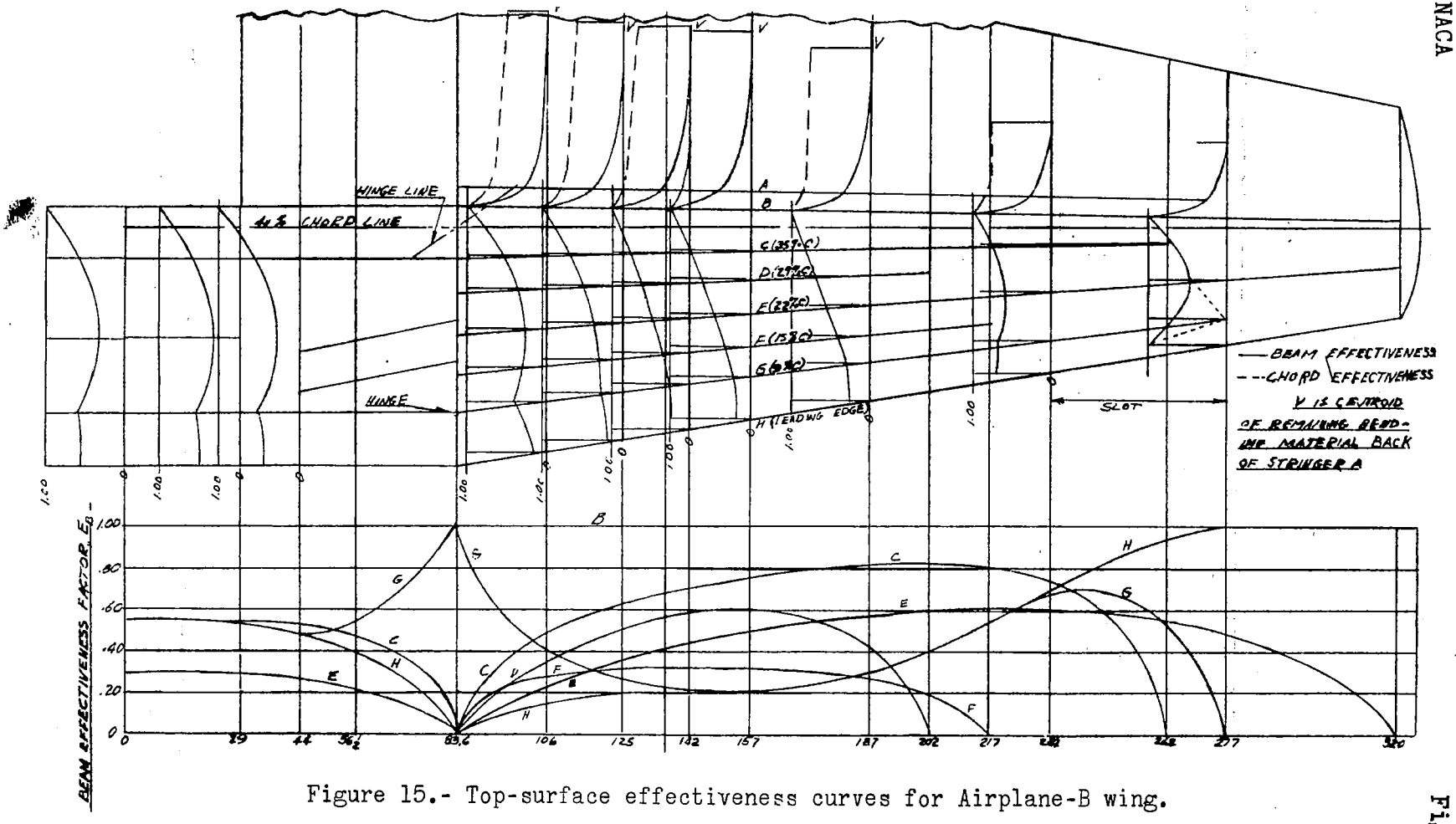

Figure 15.- Top-surface effectiveness curves for Airplane-B wing.

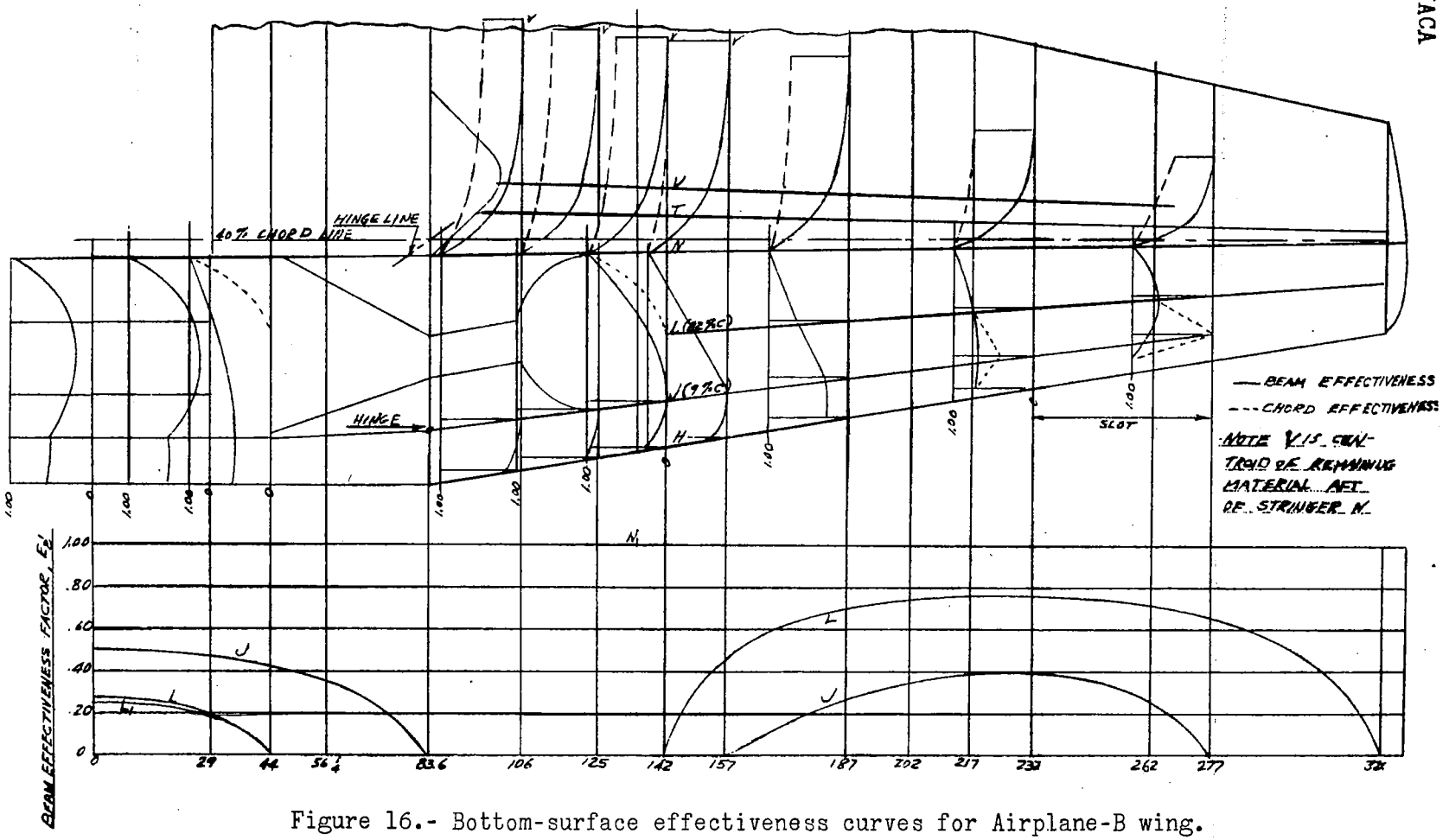

Figure 16.- Bottom-surface effectiveness curves for Airplane-B wing.

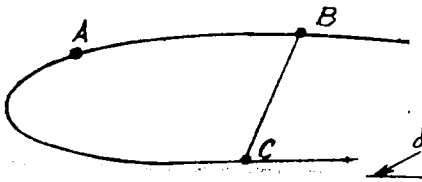

Figure 17.— Hinge fittings.

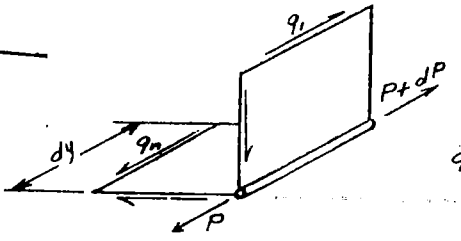

Figure 18.

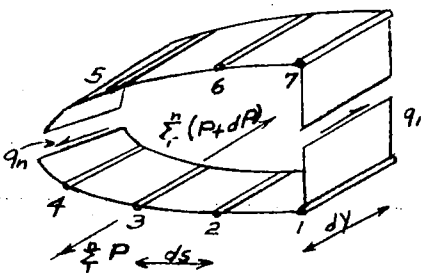

Figure 19.

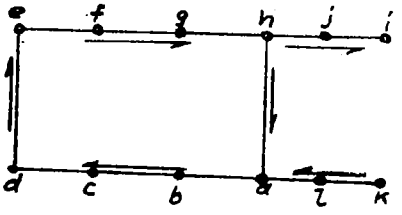

Figure 20.

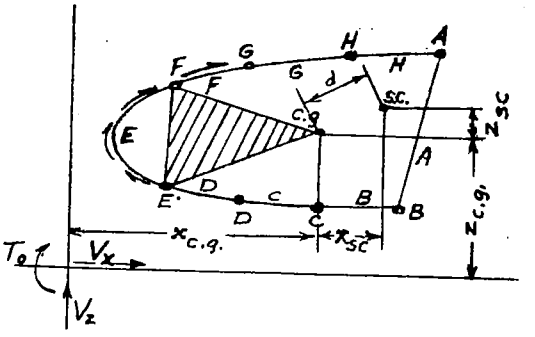

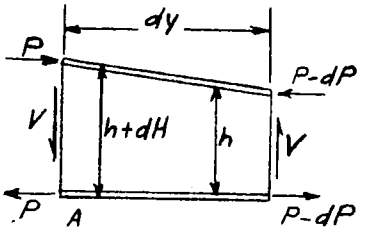

Figure 22.

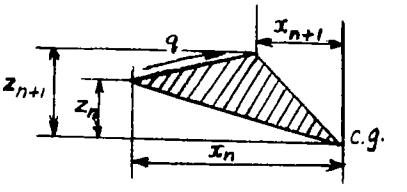

Figure 21.—Location of shear center. The center of gravity is any convenient point, usually centroid of material effective in bending.

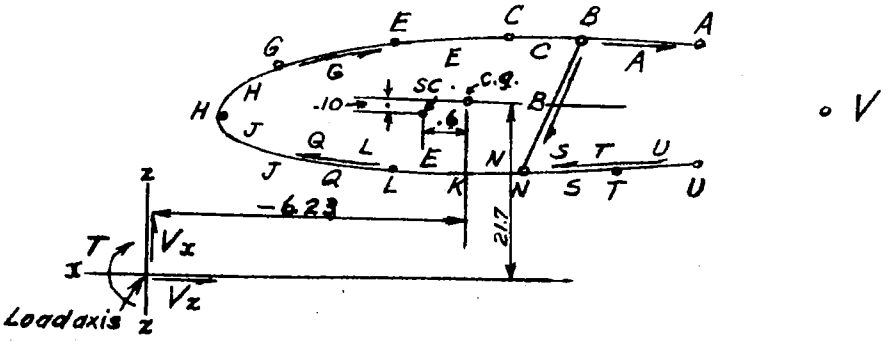

Figure 23.— Sign convention. All loads and dimensions shown are positive.

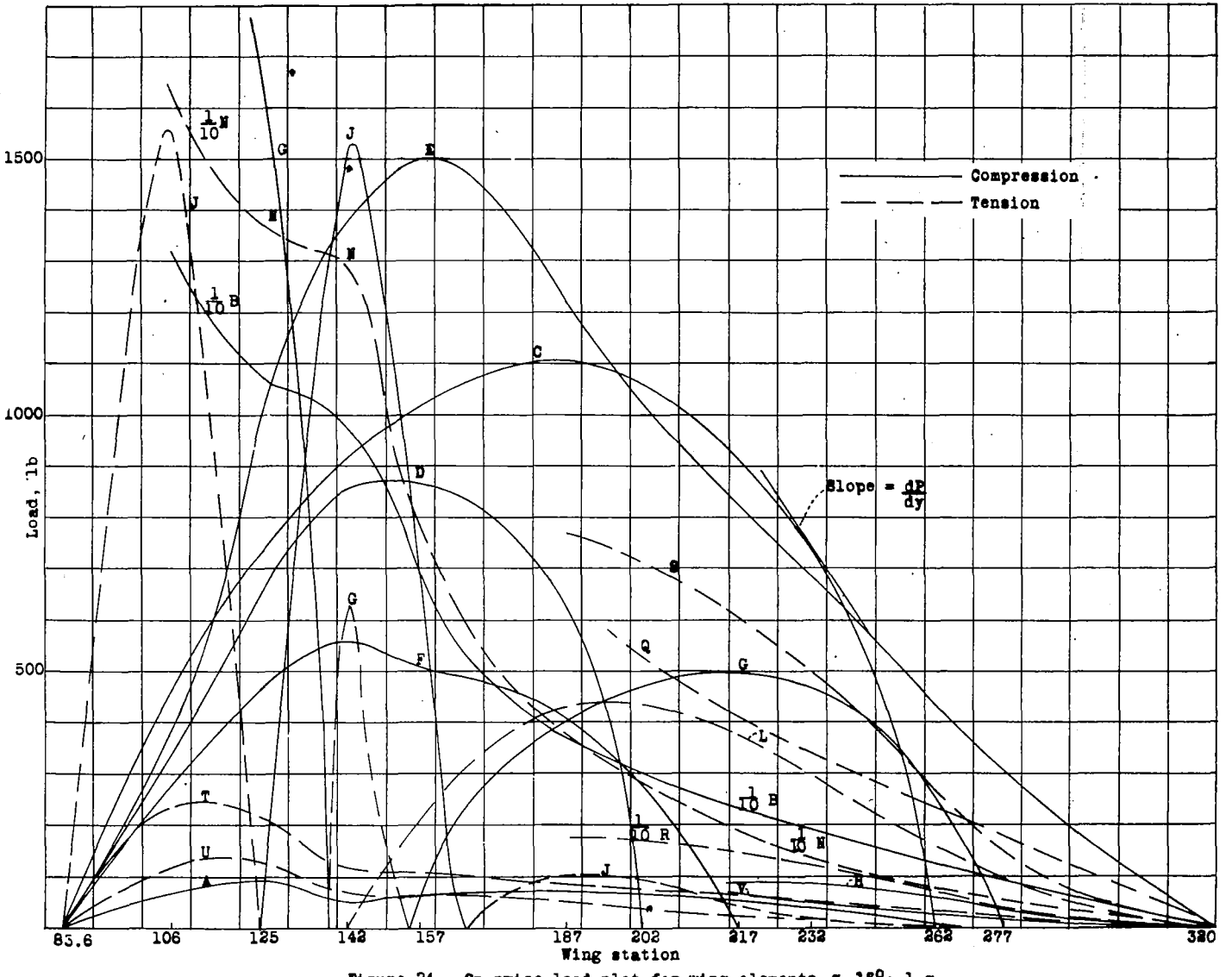

Figure 24.- Spanwise load plot for wing elements. α ,15°; 1 g.

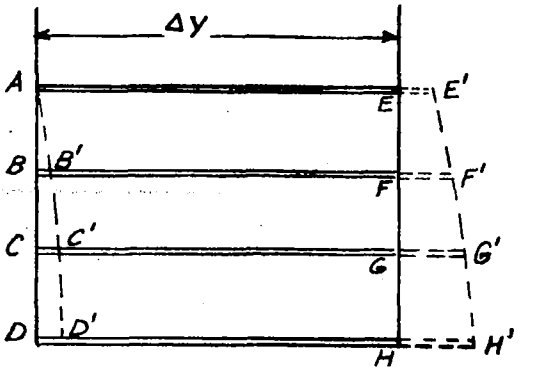

Figure 25.

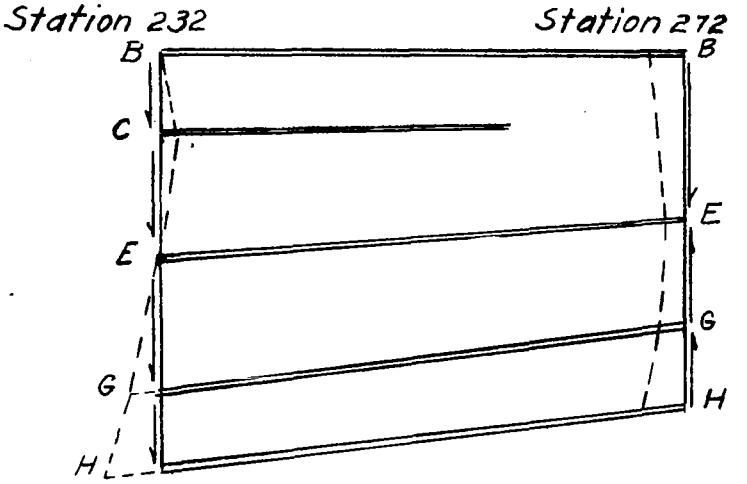

Figure 26.-Deformation from B, station 232 to H, station 277.

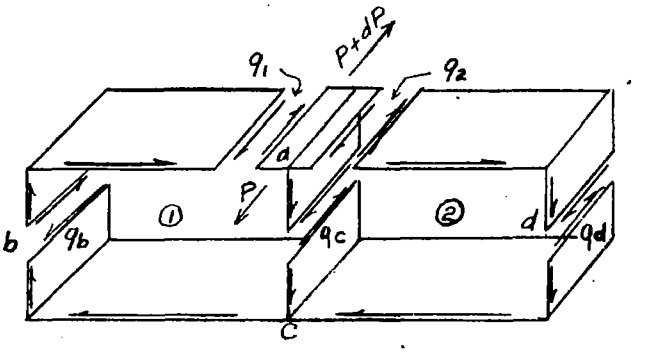

Figure 27.-
(See reference 12.)